HICCUP: Bit Interleaved Coded Modulation designed for multiple antenna channels with iteration joint detection and decoding

Joseph Boutros and Nicolas Gresset

Communications and Electronics Department
ENST, 46 Rue Barrault, 75013 PARIS, France

{boutros,gresset}@enst.fr

July 15, 2003

Comments on this HICCUP report

This report gathers the majority of results obtained by GET/ENST under the European project HICCUP. This report corresponds to the three following deliverables:

1- Close to capacity performance.
2- Receiver Interface.
3- Space-time code selection.

The first two objectives are fully attained as described in this document, see sections 4.3, 4.4 and 4.5. The third objective is also attained as described in sections 3.2, 3.3 and 3.4. The list of publications related to this project is:
1- "Soft-input soft-output lattice sphere decoder for linear channels," by Joseph Boutros, Nicolas Gresset, Loïc Brunel and Marc Fossorier, *IEEE Global Communications Conference*, San Francisco, December 2003.
2- "Soft Output Detection for Multiple Antennas: accelerated sphere decoding and shifted list enumeration," by Joseph Boutros, Nicolas Gresset, Loïc Brunel and Marc Fossorier, *Gretsi Conference*, Paris, September 2003.
3- "Turbo coding and decoding for multiple antenna channels," by Joseph Boutros, Nicolas Gresset and Loïc Brunel, *International Symposium on Turbo Codes*, Brest, September 2003.
4- "Genie closed-form performance on MIMO channels and its application to mapping optimization for joint detection and decoding", by Nicolas Gresset, Joseph Boutros and Loïc Brunel, submitted to the *IEEE Transcations on Communications*.

Contents

List of Tables

List of Figures

1 Introduction

This document is dedicated to the design and performance analysis of bit-interleaved coded modulations for multiple antenna channels, i.e., multiple-input multiple-output (MIMO) channels. Channel coding techniques for MIMO channels, commonly known as space-time coding, can be classified into four major categories:

• Multi-dimensional trellis coded modulations (TCM) [42][39].

This category includes Ungerboeck-like coded modulations and the simple case of a classical convolutional code where each trellis transition is associated to one channel use.

• Space-time block coding (STBC).

The latency of STBC is minimal compared to other techniques. This category includes orthogonal and quasi-orthogonal designs (OD and QOD) [40][27] and the simple technique proposed by Alamouti [2].

• Multilevel coding (MLC) for multiple antennas.

Since the original work by Imai and Hirakawa [26][46], it has been demonstrated that MLC can be applied to any type of channels, i.e., scalar and vector channels. In MIMO channels, different levels for coding are defined on QAM symbols fed at the channel input or directly on the binary labels of those symbols.

• Bit-interleaved coded modulations.

Combining the original ideas by Zehavi [49][16], Berrou & Glavieux [7], a coded modulation is built by cascading a convolutional code, a pseudo-random interleaver, a QAM symbol mapper and a MIMO channel. The receiver starts by an APP detection of the multiple antenna channel followed by a SISO decoding of the convolutional code. The latter procedure is iterated a finite number of times, where the convolutional code extrinsics are fed back as a priori information to the APP detector [12][37].

2 System model and parameters

Most of digital transmission systems can be modeled by a lattice sphere packing [19][1][15]. As a non-exhaustive list we cite multiple antenna (MIMO) channels, synchronous code division multiple access, inter-symbol interference channels, etc. In the sequel, we will focus on bit-interleaved coded modulations (BICM) transmitted on MIMO channels [22][39]. The receiver is supposed to perform soft-input soft-output (SISO) iterative detection and decoding. Our study may be easily adapted to any system that allows a lattice representation.

We consider an ergodic frequency non-selective Rayleigh fading channel with n_t transmit antennas and n_r reception antennas. It is assumed that $n_t = n_r$ for simplicity reasons. Each reception antenna is perturbed by an additive white complex Gaussian noise η_j, $j = 1 \dots n_r$, with zero mean and variance $2N_0$. The channel path connecting antenna i to antenna j has a complex Gaussian distributed gain h_{ij}, where $E[h_{ij}] = 0$, $E[|h_{ij}|^2] = 1$, $i = 1 \dots n_t$ and $j = 1 \dots n_r$. Here, the symbol $E[.]$ denotes mathematical expectation. The

MIMO channel coefficients h_{ij} are supposed to be statistically independent. As usual, the MIMO channel will be represented by its $n_t \times n_r$ matrix $H = [h_{ij}]$.

The two following classical channel models are considered hereafter:

- **Ergodic (non-static) fading channel**: the channel matrix H changes from one symbol period to another. We say that the channel coherence time is $T_{\text{coh}} = 1$.
- **Block fading (quasi-static) channel**: the channel matrix H is constant during a burst of length $T_{\text{coh}} > 1$, e.g., $T_{\text{coh}} = 100$.

The channel input-output relation is

$$y = zH + \eta \tag{1}$$

where $y \in \mathbb{C}^{n_r}$, and the channel input $z \in \mathbb{C}^{n_t}$ is defined as $z = (z_1, \ldots, z_{n_t})$. The symbols z_i belong to an M-QAM constellation [33].The transmitter structure is illustrated in Fig. 1. The information binary elements are encoded by a rate R_c convolutional code. The coded bits $\{c_\ell\}$ are randomly interleaved and fed to a M-QAM mapper ($M = 2^m$) that generates z. The spectral efficiency of the system is $R_c \times m \times n_t$ bits per channel use, or equivalently, $R_c \times m$ bits/sec/Hz.

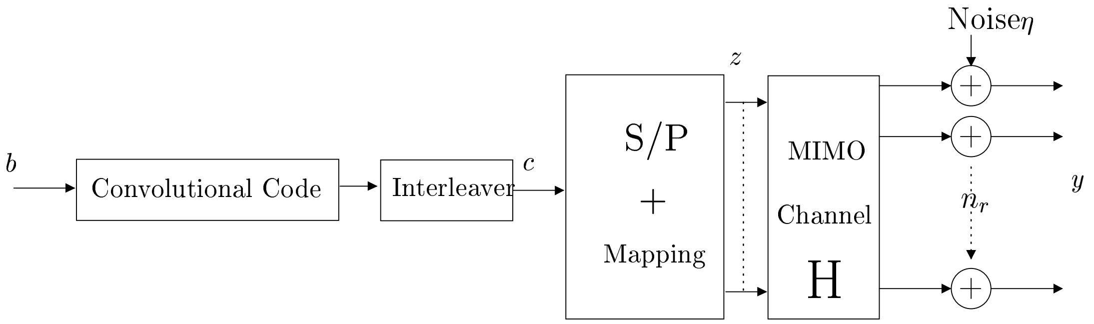

Figure 1: Classical transmitter model (BICM)

An iterative joint detection and decoding receiver is based on the exchange of soft values between the SISO QAM-detector and the SISO convolutional decoder. The SISO detector computes the extrinsic probabilities $\xi(c_\ell)$ via a classical sum product expression including the conditional likelihoods $p(y/z)$ and the a priori probabilities $\pi(c_\ell)$ fed back from the SISO decoder. The SISO detector computes the extrinsic information, which corresponds to the extrinsic probability that the j^{th} coded bit equals 1, as given in the following normalized marginalization:

$$\xi(c_\ell) = \frac{\sum_{z' \in \Omega(c_\ell = 1)} \left[\left(e^{-\frac{\|y - z'H\|^2}{2\sigma^2}} \right) \prod_{r \neq \ell} \pi(c_r) \right]}{\sum_{z \in \Omega} \left[\left(e^{-\frac{\|y - zH\|^2}{2\sigma^2}} \right) \prod_{r \neq \ell} \pi(c_r) \right]} \tag{2}$$

where Ω is the Cartesian product $(M\text{-QAM})^{n_t}$, i.e., the set of all vectors z generated by the QAM mapper, $|\Omega| = 2^{mn_t}$. The subset $\Omega(c_\ell = 1)$ is restricted to the vectors z where the l^{th} bit is equal to 1. By exploiting the trellis structure of the code, the SISO decoder computes the soft values (a posteriori and extrinsic probabilities) for the coded bits using the Forward-Backward algorithm [3]. The information exchange between inputs and outputs of the two blocks is shown on Fig. 2.

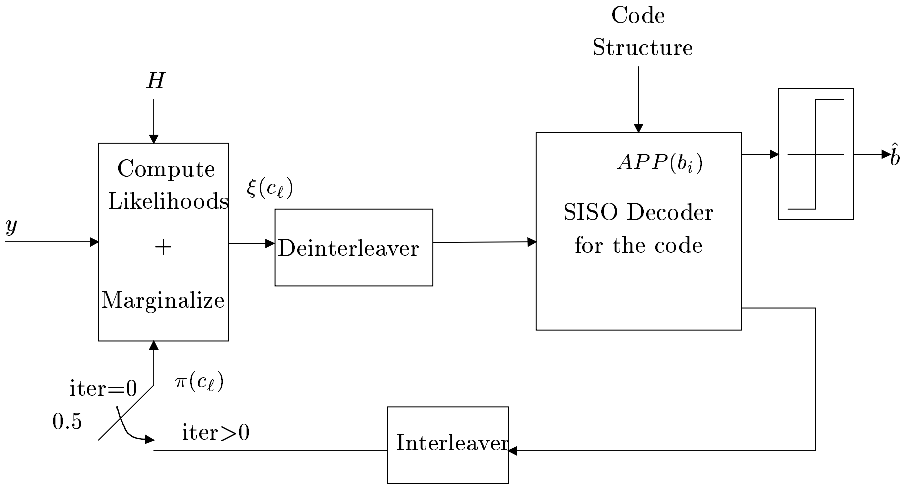

Figure 2: Joint detection and decoding system

Consider the iterative detection and decoding process of the BICM transmitted on the multiple antenna channel as illustrated in Fig. 1 and 2. Assume that extrinsic information associated to such a process is converging toward a limit. The best limit corresponds to the ideal situation where the extrinsic information is perfectly reliable, i.e, $\pi(c_\ell) = c_\ell \in \{0, 1\}$. This is called the *genie* situation. The expression of the detector soft value, when the a priori is fed back by a genie, is easily obtained from (2):

$$\xi(c_\ell) = \frac{e^{-\|y-zH\|^2/2N_0}}{e^{-\|y-zH\|^2/2N_0} + e^{-\left\|y-\bar{z}^\ell H\right\|^2/2N_0}} \tag{3}$$

where $\bar{z}^\ell$ is produced by complementing the ℓ^{th} bit in the binary labeling of z. Obviously, from the definition of $\xi(c_\ell)$ in (2), the binary element in the ℓ^{th} position is equal to 1 (respectively 0) in z (respectively $\bar{z}^\ell$). In this case, the system is equivalent to a multidimensional binary modulation BSK with signaling alphabet $\left\{z, \bar{z}^\ell\right\}$ transmitted on a $1 \times n_r$ single input, multiple output (SIMO) channel. We are interested in evaluating the error probability P_e at the detector output when the genie is active. This error probability is directly related to the decision making on $\xi(c_\ell)$. By conditioning on the channel state H and the transmitted QAM vector z, we can write

$$P_{e|H,z} = E_\ell \left[P\left(|\xi(c_\ell) - c_\ell| \geq 0.5\right)\right] \tag{4}$$

The symbol $E_\ell[.]$ denotes mathematical expectation over the position ℓ of the coded bit. Then, using (3) and (4), we can express P_e with a classical inequality including H, z and η:

$$P_e = E_{H,z,\ell}\left[P\left(\left\|(z-\bar{z}^\ell)H+\eta\right\| \leq \|\eta\|\right)\right] \tag{5}$$

which is equal to

$$P_e = E_{H,z,\ell}\left[Q\left(\sqrt{\frac{\|(z-\bar{z}^\ell)H\|^2}{4N_0}}\right)\right] \tag{6}$$

The norm $\left\|(z-\bar{z}^\ell)H\right\|^2$ is calculated from

$$\left\|(z-\bar{z}^\ell)H\right\|^2 = \sum_{u=1}^{n_r}\left|\sum_{v=1}^{n_t}(z_v - \bar{z_v}^\ell)h_{vu}\right|^2 \tag{7}$$

We can remark that the performance of the system at the input of the decoder, when the apriori feedback at the input of the detector is perfect, is the average probability of the $|\Omega| \times m \times n_t$ equivalent BSKs with distance $d(z, \bar{z}^\ell)$ on a $n_t \times n_r$ MIMO channel. If z and $\bar{z}^\ell$ belong to the same antenna, which is generally the case, this leads to the performance evaluation of a BSK modulation on a $1 \times n_r$ MIMO channel.

3 Transmitter study and design

3.1 BSK performance on $1 \times n_r$ MIMO channel

All the performance presented in this document lie on the performance of a Binary Shift Keying (BSK) on a $1 \times n_r$ MIMO channel. The BSK is defined by two equiprobable symbols z and $\bar{z}$, their euclidean distance is defined by $d(z, \bar{z})$. Without loss of generality, let us suppose the symbol z to be transmitted, the received symbol y is given by

$$y = zh + \eta. \tag{8}$$

where h is column vector defining the $1 \times n_r$ MIMO channel.
We define the distance $d(z, \bar{z}) = \left\|z - \bar{z}^\ell\right\|$. The quadratic distance between the two symbols filtered by the channel is $d(z, \bar{z})^2\|h\|^2$. The squared Euclidean norm $\|h\|^2$ has a central χ^2 distribution with degree $2n_r$, the real gaussian random variables have zero mean and variance 1/2 :

$$p_{\|h\|^2}(r) = \frac{1}{(n_r-1)!}.r^{n_r-1}e^{-r}, \quad r \geq 0 \tag{9}$$

The noise is white gaussian distributed, the symbols equiprobable, so we can deduce :

$$P_e = \Phi\left(d(z, \bar{z})^2\right) \tag{10}$$

The function $\Phi(.)$ is defined as:

$$\Phi\left(d(z,\bar{z})^2\right) = E_h\left[Q\left(\sqrt{\frac{d(z,\bar{z})^2\left\|h\right\|^2}{4N_0}}\right)\right] \tag{11}$$

The error probability P_e can be calculated in a closed-form expression as on a $2n_r$-diversity Rayleigh fading channel (see chap.14 in [33]). The general expression given in (10) becomes:

$$P_e = \Phi\left(d(z,\bar{z})^2\right) = \left(\frac{1-\frac{1}{\sqrt{1+8N_0/d(z,\bar{z})^2}}}{2}\right)^{n_r}\sum_{k=0}^{n_r-1}\begin{pmatrix} n_r-1+k \\ k \end{pmatrix}\left(\frac{1+\frac{1}{\sqrt{1+8N_0/d(z,\bar{z})^2}}}{2}\right)^{k} \tag{12}$$

3.2 Space-Time Code optimization for BICM-ID

Time spreading matrices such as Space-Time codes or Rotations are used to exploit diversity on fading channels spreading the symbols in time and space. In a MIMO channel, the n_t transmit and n_r reception antennas create the transmission and reception diversity, respectively. When spreading the symbols over different symbol times, the transmitter generates a time diversity. The maximum diversity achievable for such a system is equal to the product of the three diversity. We will see later the conditions that allow to observe the maximum diversity.
Clearly, the transformation has to be full rank to exhibit full-diversity. Indeed, a non-full rank transformation is equivalent to a reduction of the number of reception antennas. An other proposition to be verified by the spreading matrix is the norm conservation...
Let us define n_s the number of complex dimensions of the spreading matrix S. The integer $s = n_s/n_t$ is called the spreading factor of the transformation, it gives the number of time symbols that are mixed together.
In Space Time Code Theory, we use to consider block fading channels, i.e. we have c channel observations for one spreading Matrix, the channel stay constant during s/c channel use. The equivalent $n_t.s \times n_r.s$ channel matrix is defined by a bloc diagonal matrix which elements are the observed channel matrices $H_i, i \in [1..c]$ each repeated s/c times.

$$H = diag\{\underbrace{H_1,\ldots,H_1}_{s/c},\underbrace{H_2,\ldots,H_2},\ldots,\underbrace{H_c,\ldots,H_c}\} \tag{13}$$

We will first consider the ergodic case when $c = s$ and derive the condition that ensure maximum diversity, under these conditions, the genie performance is independent of the choice of the matrix S. Then we will consider the general case of block fading MIMO channel with parameter c.

3.2.1 Space Time codes for the Ergodic MIMO channel

When the channel changes at each channel use, i.e. when $c = s$, it is said to be ergodic. In this case, the channel matrix when using a $n_t.s \times n_r.s$ spreading matrix is block diagonal $H = diag\{H_1, \dots, H_s\}$, of which diagonal elements are the MIMO channel matrices of the s consecutive time period. Equivalently, $z = \{z_1, \dots, z_s\}$ is a vector built from the concatenation of the s consecutive n_t-length vectors. We build x the noiseless filtered vector, η the noise vector and y the received vector in the same manner.
We can now write :

$$y = zSH + \eta \tag{14}$$

First, we can remark that if $s = 1$, the elements of the matrix $H' = SH$ are centered complex gaussian distributed with variance 1, indeed

$$m_{ij} = \sum_{k=1}^{n_s} s_{ik} H_{kj} \sim \mathcal{N}\left(0, \sum_{k=1}^{n_s} s_{ik}^2\right) \tag{15}$$

and from the energy conservation proposition of the transformation, we have $\sum_{k=1}^{n_s} s_{ik}^2 = 1$. In this case, the spreaded MIMO channel can be seen as an other realization of a simple MIMO channel, the $s = 1$ spreading matrices are unusefull in terms of asymptotic performance.
We will calculate the performance of this system at the output of the detector when the apriori feedback is perfect and when $s > 1$. Let us consider the ℓ-th coded bit c_ℓ of the transmitted vector z. Without loss of generality (see the section on multi dimensional mappings), we consider here that z and $\bar{z}^\ell$ belong to the same QAM symbol indexed by the integer i. We can deduce i from

$$i = \left\lceil \frac{l}{m} \right\rceil \tag{16}$$

In the whole document, all the integers i are defined this way. For a given $z \in \Omega$ and $\ell \in [1..m.n_t]$, let us consider

$$\|(z - \bar{z}^\ell)SH\|^2 = d(z, \bar{z}^\ell)^2 \sum_{u=1}^{n_s} \left| \sum_{v=1}^{n_s} s_{iv} h_{vu} \right|^2 \tag{17}$$

The matrix H is block diagonal, the size of each block is $n_t \times n_r$, we have

$$\|(z - \bar{z}^\ell)SH\|^2 = d(z, \bar{z}^\ell)^2 \|S_i H\|^2 = d(z, \bar{z}^\ell)^2 \sum_{t=0}^{s-1} \sum_{u=1}^{n_r} \left| \sum_{v=1}^{n_t} s_{i,v+t.n_t} h_{v,u,t} \right|^2 \tag{18}$$

where $h_{.,.,t}$ make reference to the coefficients of the t-th channel observation, i.e. $h_{i,j,t} = h_{i+t.n_t, j+t.n_t}$. We can remark that

$$\forall t \in [0..s-1], \forall u \in [1..n_r], \sum_{v=1}^{n_t} s_{i,v+t.n_t} h_{v,u,t} \sim \mathcal{N}\left(0, \frac{1}{2} \sum_{v=1}^{n_t} |s_{i,v+t.n_t}|^2\right) \tag{19}$$

The distribution of $\|S_iH\|^2$ is a generalized chi-square composed by n_s gaussian distributions. The variance of these gaussian distributions are not equal in most of the cases, that is why closed form expressions are not available. In the general case there are s different variance values, each being the variance of n_t gaussian distributions. It is very important to remark that two spreading transformations A and B satisfying the same norm proposition

$$\forall t \in [0..s-1], \sum_{v=1}^{n_t} |a_{i,v+t.n_t}|^2 = \sum_{v=1}^{n_t} |b_{i,v+t.n_t}|^2 \tag{20}$$

lead to the same genie performance, i.e. the same coded performance when the system converges to the optimal fixed point. Moreover, if one of these norm is equal to 0, the system performance loose one degree of diversity, the matrices leading to such non-optimality are not considered here.
We can derive a first construction proposition:
proposition 1: If all the norms of the 1/s-th parts of the lines of a $\mathbf{n_t}.s \times \mathbf{n_r}.s$ spreading matrix are equal, the maximum diversity $\mathbf{n_r} * \mathbf{s}$ is observed at the output of the detector of a BICM-ID on a $\mathbf{n_t} \times \mathbf{n_r}$ MIMO channel.
In this case, when $\forall t \in [0..s-1], \sum_{v=1}^{n_t} |s_{i,v+t.n_t}|^2 = 1/s$, the considered distribution is chi-square with degree $2.n_r.s$ and parameter $n_t/(2n_s) = 1/(2s)$.

$$p_{\|S_iH\|^2}(r) = \frac{(sr)^{sn_r-1}}{(sn_r-1)!}.s.e^{-s.r}, \quad r \geq 0 \tag{21}$$

We can see the distributions of the norms of the equivalent BSKs on Fig 3,4 and 5. As an example of transformation verifying the norm proposition for every value of s, we have cyclotomic rotations since $|s_{ij}|^2 = 1/n_s$.
If we set the noise variance to N_0 calculated for the n_r reception antennas, let us consider the law of the modulus of a line of an ergodic MIMO channel with $s.n_r$ reception antennas, with noise variance normalization $s.N_0$ due to the $s.n_r$ reception antennas, $p_{\|h_{s.n_r}\|^2/(s.N_0)}(r)$, we can observe the equality

$$p_{\|S_iH\|^2/N_0}(r) = s.p_{\|h_{s.n_r}\|^2/(s.N_0)}(s.r) = p_{\|h_{s.n_r}\|^2/N_0}(r) \tag{22}$$

We can observe that we have the same reception diversity and performance between an ergodic channel with n_r reception antennas and time spreading factor equal to s and an ergodic channel with $s.n_r$ reception antennas and no time spreading.

3.2.2 Quasi-static MIMO channel

In the case when the spreading matrix only see $c = 1$ channel observation, the same fixed $n_t \times n_r$ matrix $H_f = h_{u,v}$ is applied to the vectors $\forall t \in [0 \ldots s-1], \quad \{s_{i,t.n_t}, \ldots, s_{i,(t+1).n_t}\}$, we can write

$$\|(z-\bar{z}^\ell)SH\|^2 = d(z,\bar{z}^\ell)^2 \sum_{t=0}^{s-1} \sum_{u=1}^{n_r} \left| \sum_{v=1}^{n_t} s_{i,v+t.n_t} h_{v,u} \right|^2 = d(z,\bar{z}^\ell)^2 \sum_{t=0}^{s-1} \sum_{u=1}^{n_r} |G_{t,u}|^2 \tag{23}$$

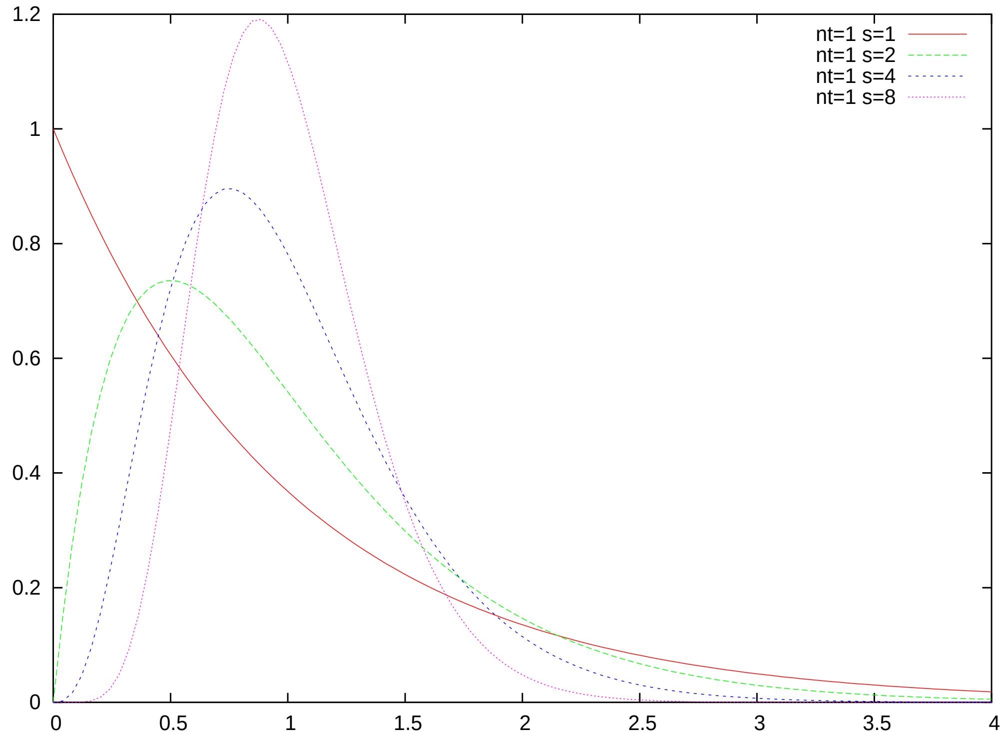

Figure 3: Law of the norm of the equivalent BPSK

with $G_{t,u} = \sum_{v=1}^{n_t} s_{i,v+t.n_t} h_{v,u}$.

The law of $\|(z - \bar{z}^\ell)SH\|^2$ is a chi-square-like distribution of the norm of the set of correlated gaussian $G_{t,u}$. If we want to observe the maximal diversity, we have to choose the matrix S properly. We can first remark that

$$\forall (t,t') \in [0..s-1]^2, \forall (u,u') \in [0..n_r]^2, \quad u \neq u' \Rightarrow E\left[G_{t,u} G^*_{t',u'}\right] = 0 \tag{24}$$

because the elements of two different column of H_f are uncorrelated.
let us consider the case when $u = u'$:

$$\forall (t,t',u), E\left[G_{t,u} G^*_{t',u}\right] = E\left[\left(\sum_{v=1}^{n_t} s_{i,v+t.n_t} h_{v,u}\right)\left(\sum_{v=1}^{n_t} s_{i,v+t'.n_t} h_{v,u}\right)^*\right] \tag{25}$$

Since $\forall v \neq v', E\left[h_{v,u} h^*_{v',u}\right] = 0$ we obtain the new proposition

$$\forall (t,t',u), E\left[G_{t,u} G^*_{t',u}\right] = 0 \Leftrightarrow \sum_{v=1}^{n_t} s_{i,v+t.n_t} s^*_{i,v+t'.n_t} = 0 \tag{26}$$

proposition 2: If the 1/s-th parts of the lines of a $\mathbf{n_t.s \times n_r.s}$ spreading matrix are orthogonal with equal norm, the maximum diversity $\mathbf{n_r * s}$ is observed at the output of the detector of a BICM-ID on a quasi-static $\mathbf{n_t \times n_r}$ MIMO

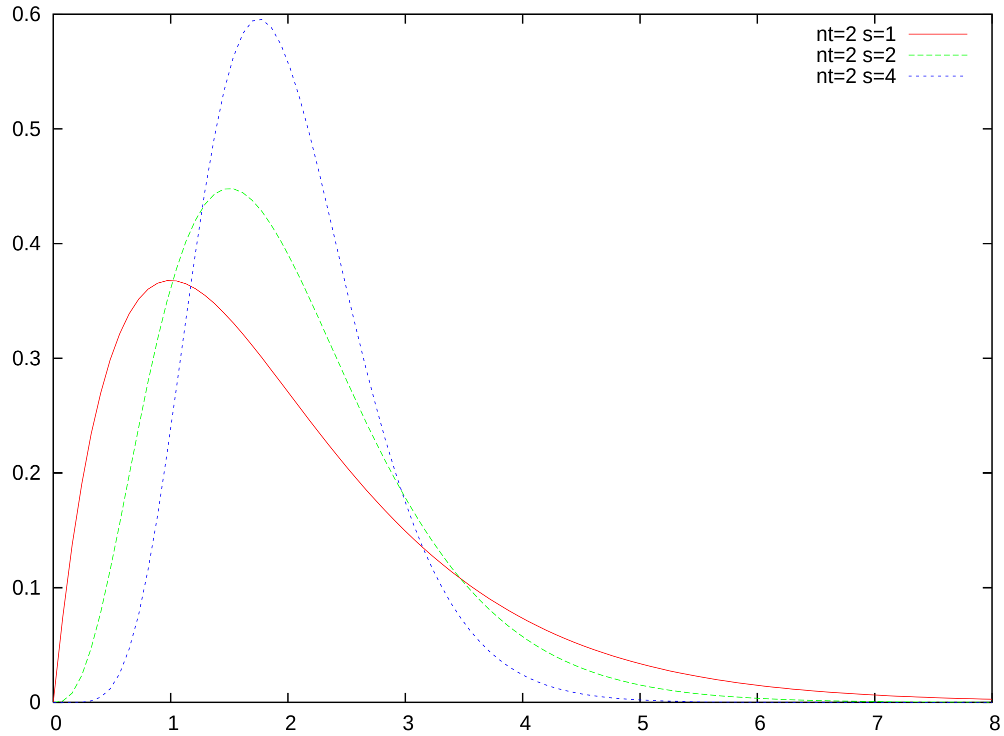

Figure 4: Law of the norm of the equivalent BPSK

channel.

For example, we can take a $n_t \times n_t$ rotation matrix Θ and concatenate s of this lines to form a $n_t.s$-length vector which satisfies the proposition 2. Here we see again that we must have $s \leq nt$.

In the case when proposition 2 is satisfied, the distribution is equal to the one described in eq (21), hence we have the same performance as a an ergodic MIMO channel with n_r reception antennas ans a time spreading factor s, and the same performance as an ergodic MIMO channel with $s.n_r$ reception antennas.

3.2.3 Block fading MIMO channel

In the general case, when a spreading matrix encounters c channel observations, the same matrix H_w is applied to the vectors $\forall t \in [1 \dots s/c], \quad \left\{ s_{i,v+(w.s/c+t).n_t}, \dots, s_{i,v+(w.n/c+t).(n_t+1)-1} \right\}$ we can write

$$\|(z - \bar{z}^\ell)SH\|^2 = d(z, \bar{z}^\ell)^2 \sum_{w=0}^{c-1} \sum_{t=0}^{s/c-1} \sum_{u=1}^{n_t} |G_{t,u,w}|^2 \tag{27}$$

where $G_{t,u,w} = \sum_{v=1}^{n_t} s_{i,v+(w.s/c+t).n_t} h_{v,u,w}$ have a gaussian distribution. Again, we can remark that for two different values of w or u the gaussian distributions are uncorrelated since they are summation of independent gaussian variable belonging to different channel

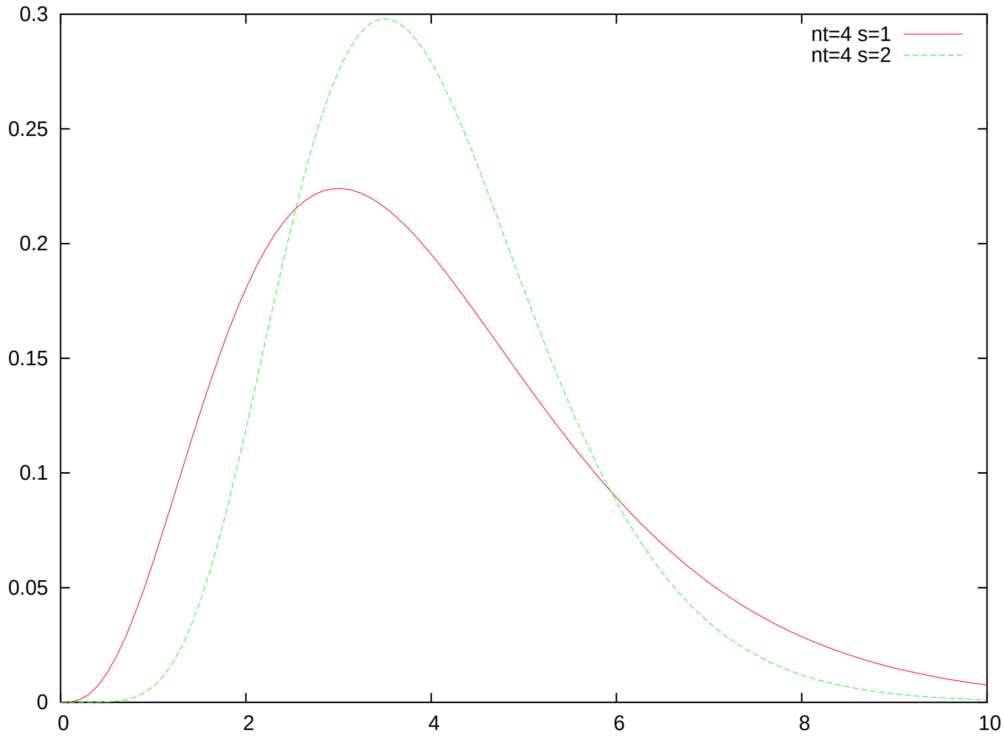

Figure 5: Law of the norm of the equivalent BPSK

observations or different columns of one channel observation matrix. The decorrelation criterion becomes :

$$\forall(t,t',u,w), E\left[G_{t,u,w}G^*_{t',u,w}\right] = 0 \Leftrightarrow \sum_{v=1}^{n_t} s_{i,v+(w.n/c+t).n_t} s^*_{i,v+(w.n/c+t').n_t} = 0 \qquad (28)$$

We remark here that we can consider the block fading MIMO channel as an ergodic channel composed of c channel observations, each of these channel observations being a quasi-static channel of one $n_t \times n_r$ MIMO channel observation repeated s/c times.

Proposition 3 :

For the construction of a space time code for BICM-ID on $\mathbf{n_t} \times \mathbf{n_r}$ block fading channels with c different channel observations and a time spreading factor equal to s, we can apply a $(\mathbf{s/c.n_t} \times \mathbf{s/c.n_t})$ space time spreading matrix that maximize the diversity for quasi-static channels (proposition2) on the time symbols that observe the same channel, and then apply a general $(\mathbf{s.n_t} \times \mathbf{s.n_t})$ space time spreading matrix that maximizes the diversity for ergodic channels (proposition1).

In these conditions, the maximum diversity at the output of the detector for a given s and c is $s/c.n_r.c = s.n_r$ where $s/c \leq n_t$. The maximal diversity that can be achieved is obtained in the case when $s/c = n_t$, in this case the diversity at the output of the detector is $c.n_t.n_r$. Let us suppose that a codeword of the BICM see N_c different channel observations, the interleaver of the BICM should ensure that the blocks of s consecutive time period should see $min(n_t, N_c)$ to ensure maximum diversity at the output of the detector.

3.2.4 Construction of an optimized Space Time Block Code for BLOCK Fading MIMO channels

Let us consider a $nt \times n_r$ block fading MIMO channel with time spreading factor equal to s and c different channel observations per spreading matrix. Cyclotomic rotations are very useful complex rotation with an algebraic construction [11]. Thanks to proposition 1, 2 and 3, we can deduce the following construction points :

- Let us define Ξ a $n_s \times n_s$ cyclotomic rotation matrix. Its coefficients are defined by

$$\Xi_{u,v} = \frac{1}{\sqrt{n_s}} exp\left(2j\pi(u-1)\left(\frac{1}{\Phi^{-1}(2n_s)} + \frac{v-1}{n_s}\right)\right) \tag{29}$$

  where $\Phi(.)$ is the Euler's function.

- Let us define a $n_t \times n_t$ rotation matrix $\Theta^{(w)}$. We can express

$$\Delta_{\Theta}^{(w)} = diag\left(\Theta_{1,1}^{(w)}, \ldots, \Theta_{1,n_t}^{(w)}, \ldots, \Theta_{s/c,n_t}^{(w)}, \ldots, \Theta_{s/c,n_t}^{(w)}\right) \tag{30}$$

  which is a $s/c.n_t \times s/c.n_t$ diagonal matrix containing the concatenation of the s/c first lines of $\Theta^{(w)}$.

- Let $\Delta = diag\left(\Delta_{\Theta}^{(0)}, \ldots, \Delta_{\Theta}^{(c)}\right)$, an optimum $n_s \times n_s$ space time code for BICM-ID can be expressed by

$$S = \Xi\Delta \tag{31}$$

We can choose $\forall w, \Theta^{(w)} = \Theta$ equal to a cyclotomic rotation, in this case, the diagonal coefficients of Δ are given by :

$$\begin{aligned} &\forall w \in [0, c-1], \forall t \in [0, s/c-1], \forall v \in [1, n_t], \\ &\Delta_{v+(w.s/c+t)n_t} = exp\left(2j\pi t\left(\tfrac{1}{\Phi^{-1}(2n_t)} + \tfrac{v-1}{n_t}\right)\right) \end{aligned} \tag{32}$$

Finally, the coefficients of S are given by :

$$\begin{aligned} &\forall u \in [1, n_s], \forall w \in [0, c-1], \forall t \in [0, s/c-1], \forall v \in [1, n_t], \\ &S_{u,v+(w.s/c+t)n_t} = \tfrac{1}{\sqrt{n_s}} exp\left(2j\pi\left[(u-1)\left(\tfrac{1}{\Phi^{-1}(2n_s)} + \tfrac{v-1+(w*s/c+t)*n_t}{n_s}\right) + t\left(\tfrac{1}{\Phi^{-1}(2n_t)} + \tfrac{v-1}{n_t}\right)\right]\right) \end{aligned} \tag{33}$$

3.3 Application to mapping optimization in joint detection and decoding systems

3.3.1 Independent labeling on each antenna

We will consider here the classical situation when a 2-dimensional (complex) labeling is applied on each antenna independently. Let us assume that the coded bit c_ℓ is transmitted on the i^{th} antenna. Then, $(z - \bar{z}^\ell)$ has only one non-null component in the i^{th} position. Thanks to (7), we have $\left\|(z - \bar{z}^\ell)H\right\| = d(z, \bar{z}^\ell).\, \|h_i\|$ where h_i is the i-th row of H. In the sequel, the integer i should be considered as a function of the integer ℓ, it can be calculated by the following expression

$$i = \left\lceil \frac{\ell}{m} \right\rceil \tag{34}$$

Hence, (12) leads to

$$P_e = \frac{1}{m.n_t.|\Omega|} \sum_{z \in \Omega} \sum_{\ell=1}^{m.n_t} \Phi\left(d(z, \bar{z}^\ell)\right) \tag{35}$$

The asymptotic expression of P_e when $N_0 \to 0$ is:

$$P_e \sim \binom{2n_r - 1}{n_r} \left(\frac{2N_0}{\alpha_\Omega}\right)^{n_r} \tag{36}$$

where α_Ω is defined by a harmonic mean:

$$\frac{1}{\alpha_\Omega^{n_r}} = \frac{1}{m.n_t.|\Omega|} \sum_{z \in \Omega} \sum_{\ell=1}^{m.n_t} \frac{1}{d(z, \bar{z}^\ell)^{2n_r}} \tag{37}$$

We can calculate the asymptotic gain of labeling Ω_2 with respect to labeling Ω_1 as follows:

$$Gain_{dB} \sim 10 \log_{10} \left(\frac{\alpha_{\Omega_2}}{\alpha_{\Omega_1}}\right) \tag{38}$$

Here, we can see that asymptotic gain only depends on the distance distribution of the equivalent BSKs. We can for example compare two M-QAM mappings together or a M-QAM mapping with a M-PSK mapping.

3.3.2 Multi-dimensional labellings

When we consider 2-dimensional labellings, the asymptotic gain optimization is limited by the $m \times n_t$ distances of 2-dimensional vectors. Clearly, vectors with more dimensions would lead to higher asymptotic gains, that is why we consider here multi-dimensional labellings. Let us define n_{map} the number of antennas linked by the labeling and consider the ℓ-th bit that belongs to the i-th group of antenna. The integer i is deduced from ℓ thanks to the expression

$$i = \left\lceil \frac{\ell}{m.n_{map}} \right\rceil \tag{39}$$

Then the vector $(z - \bar{z}^\ell)$ has n_t/n_{map} non-null components in positions $i_{min} = i$ to $i_{max} = i + n_t/n_{map} - 1$. In this conditions,

$$\left\|(z - \bar{z}^\ell)H\right\|^2 = \sum_{u=1}^{n_r} \left\| \sum_{v=i_{min}}^{i_{max}} (z_v - \bar{z_v}^\ell) h_{vu} \right\|^2 \tag{40}$$

Let us remark that

$$\sum_{v=i_{min}}^{i_{max}} (z_v - \bar{z_v}^\ell) h_{vu} \sim \mathcal{N}(0, \sigma_z^2) \tag{41}$$

where

$$\sigma_z^2 = \frac{1}{2} \sum_{v=i_{min}}^{i_{max}} \left|z_v - \bar{z_v}^\ell\right|^2 = \frac{1}{2} d(z, \bar{z}^\ell)^2 \tag{42}$$

The bit error probability expression is similar to (35)

$$P_e = \frac{1}{m.n_t.|\Omega|} \sum_{z \in \Omega} \sum_{\ell=1}^{m.n_t} \Phi\left(d(z, \bar{z}^\ell)\right) \tag{43}$$

3.3.3 Mapping optimization

The two points z and $\bar{z}^\ell$ define a binary shift keying constellation BSK. We obtain a set of BSK modulations for each mapping. Each BSK is associated to the complementation of a bit. For example, the Gray mapping and its associated BPSKs are represented in Fig. 6-a. A similar illustration for Ungerboeck mapping is presented in Fig. 6-b.

The function $\Phi(d^2)$ defined in (11) is a decreasing function of d^2, so maximizing the BSK distance improves the constellation mapping. Asymptotically, the mapping figure of merit is α_Ω defined in (37). For example, the genie performance of 16-QAM with Gray labeling and minimal euclidean distance 2.0 is

$$P_{e,gray} = \frac{24}{32}\Phi(4) + \frac{8}{32}\Phi(36) \tag{44}$$

and the genie performance of 16-QAM with Ungerboeck labeling is

$$P_{e,ungerboeck} = \tfrac{1}{32}\left[4\Phi(4) + 8\Phi(8) + 8\Phi(16) + 8\Phi(32) + 4\Phi(36)\right] \tag{45}$$

We can calculate the asymptotic gain of the Ungerboeck mapping on a 1×1 MIMO channel:

$$10 \log_{10}\left(\frac{\alpha_{ungerboeck}}{\alpha_{gray}}\right) = 10 \log_{10}\left(\frac{224}{103}\right) = 3.37dB \tag{46}$$

This proves the well known result on single antenna Rayleigh fading channel where Ungerboeck labeling gives better performance than Gray labeling at high SNR under iterative joint detection and decoding. We can conclude that the error probability with genie on $\xi(c_\ell)$ is equal to the average of the error probabilities of the embedded BSKs on the $1 \times n_r$

	Mean	Variance	Maximum
MIMO 1x1, nmap=1	3.15	0.35	7.10
MIMO 2x2, nmap=1	2.39	0.28	7.27
MIMO 2x2, nmap=2	5.65	0.04	6.75
MIMO 4x4, nmap=1	1.43	0.13	7.15
MIMO 4x4, nmap=2	3.59	0.04	4.94
MIMO 4x4, nmap=4	8.33	¡1e-3	8.57

Table 1: Statistics of random mappings

MIMO channel, the latter being equivalent to a generalized Rayleigh fading (Nakagami) channel with parameter n_r. The closed-form expression of the genie performance on MIMO $n_t \times n_r$ channels and the asymptotic gain expression (38) are very useful when designing binary mappings because of the low complexity of the search procedure. In the case of 16-QAM constellation, we can determine numerically the probability distribution of the asymptotic gain of a randomly selected binary mapping, taking the Gray mapping as reference. On Fig. 7, we can see the asymptotic gain distribution on 1×1 and 2×2 MIMO channels. Two types of mappings are shown. The first type denoted by $nmap = 1$ is a 2-dimensional binary mapping, i.e., same mapping on all transmit antennas. The second type denoted by $nmap = 2$ corresponds to a 4-dimensional binary mapping including both transmit antennas.

We listed in Table 1 the mean, variance and maximum asymptotic gain found by our search procedure. We randomly selected a large number (but not exhaustive) of 16-QAM mappings. In the case of 1×1 channel, the best mapping found gives an asymptotic gain of 7.1dB. This mapping is represented on Fig. 6-c and has no evident symmetry properties. When increasing the mapping dimensionality ($nmap > 1$), it is possible to increase the minimum Euclidean distances of the embedded BSKs. This explains why the statistical mean of the asymptotic gain improves for $nmap > 1$.

3.4 Computer simulations

Fig. (8-a) shows the performance at the output of the detector when a non-recursive non-systematic (7,5) rate 1/2 convolutional code is used on a 1×1 Rayleigh fading channel. The BICM pseudo-random interleaver size is 20000 bits. The number of soft-input soft-output detection and decoding iterations is 5. The three mappings compared are Gray, Ungerboeck and the optimized mapping. At high SNR, the performance under iterative detection and decoding attains the genie performance given in (35). The SNR threshold where the genie lower bound is reached depends on the quality of extrinsic information fed back from the SISO decoder and the binary mapping. Notice also that the improvement of the error rate at high SNR damages the performance at very low SNR.

Fig. (8-b) shows the bit error rate (BER) of the same system measured at the output of the SISO decoder. If we consider a BER equal to 3.6e-3 at the input of the decoder, we observe a BER equal to 1e-5 at its output. Once the genie bound is reached, the signal-to-noise ratio offset at the detector output between two mappings is preserved after SISO decoding. This can be easily checked by comparing Fig. (8-a) and (8-b).
These figures confirm that Gray mapping is the worst mapping at high SNR (i.e., when the performance is close to the genie performance). On the other hand, Gray mapping is the best mapping for low SNR. We deduce that the genie expression in (35) can be applied to optimize QAM mapping when using error-correcting codes working at high signal-to-noise ratio.

However, when using powerful error-correcting codes, e.g., a BER greater than 0.1 at the input of the decoder is sufficient to attain very low BER at its output, the Gray mapping is the best mapping. In this case, the first detection-decoding iteration has to be as efficient as possible. These results are confirmed on Fig. (9-a) and (9-b) where a parallel turbo code is used. The rate 1/2 turbo code constituent is the recursive systematic (7,5) convolutional code.

On Fig. 10, we compare the simple (7,5) convolutional code with Gray mapping, Ungerboeck and optimized mapping ($nmap = 1$) to the rate 1/2 turbo code with Gray mapping on 2×2 MIMO channel. We can see that the optimized mapping and convolutional code performs approximately 1.2dB from the turbo code for a BER equal to 1e-5.

On Fig. ref (11),the same comparison is made on a 4×4 MIMO channel with the Gray mapping, an optimized $nmap = 1$ mapping and an optimized $nmap = 4$ mapping with rate one half repetition code. The interleaver size is about 100000 bits. Surprisingly, the simple convolutional code combined with our 16-QAM optimized mapping performs close to the parallel turbo code. The gap is less than 1.0 dB at 10^{-5}. When using the optimized $nmap = 4$ mapping, too powerful codes leads to late convergence, that is why we chose to combine it with a repetition code. Surprisingly, the gain obtained after convergence is not so bad when taking into account the correction capacity of the code, with the advantage of the high complexity reduction of the soft decoder.

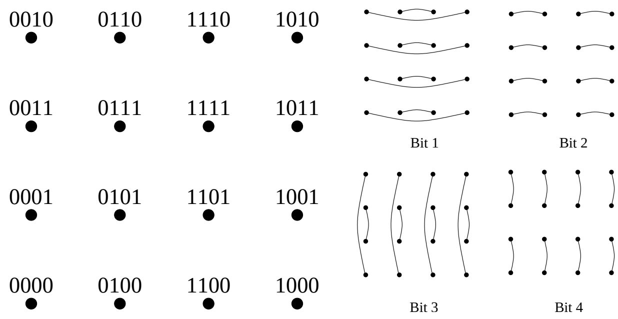

(a) Gray mapping

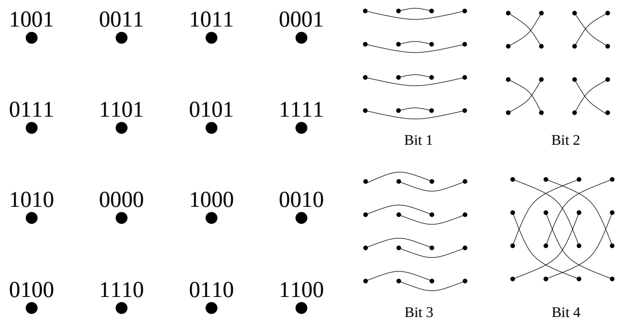

(b) Ungerboeck mapping

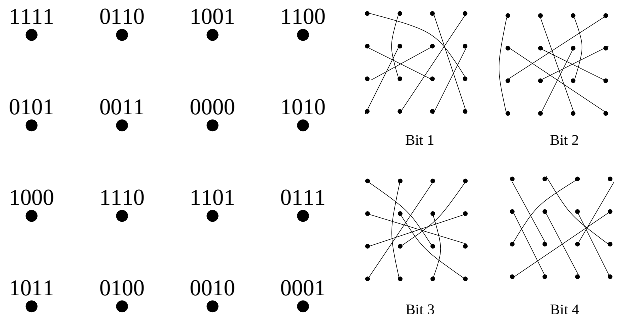

(c) Optimized mapping

Figure 6: Three mappings of 16-QAM constellation.

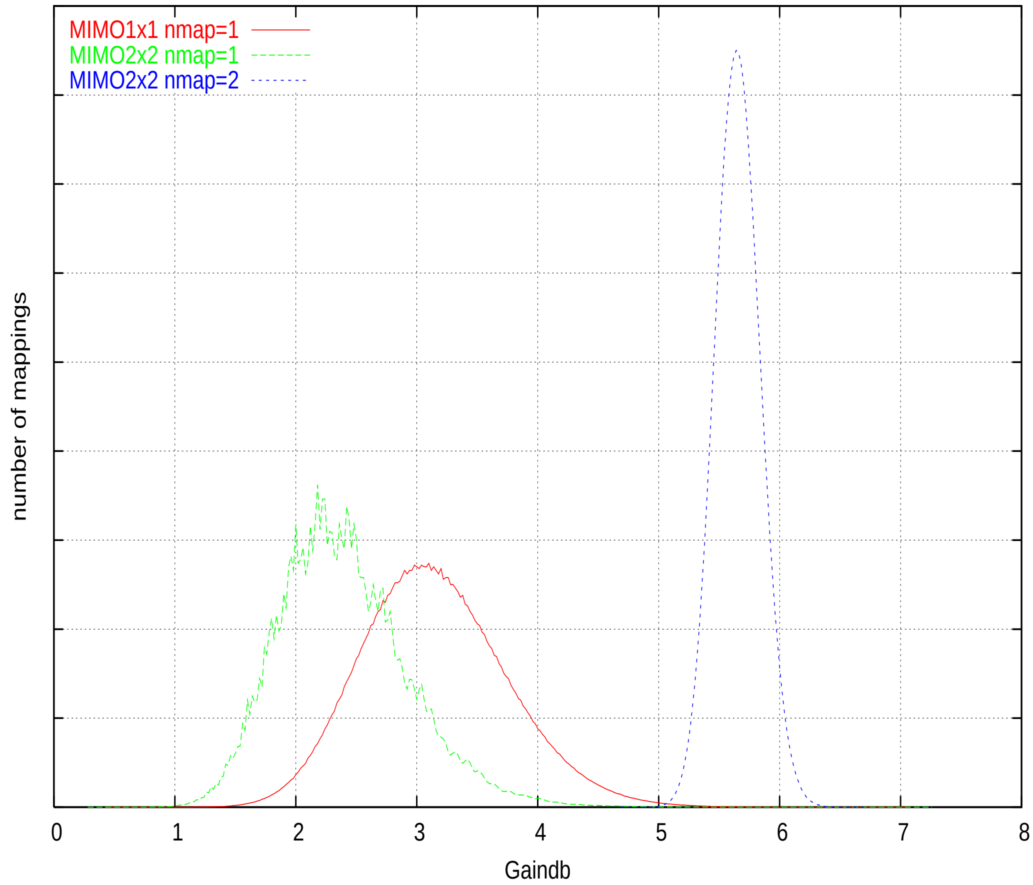

Figure 7: Asymptotic gain distribution of random mapping wrt Gray mapping, 16-QAM.

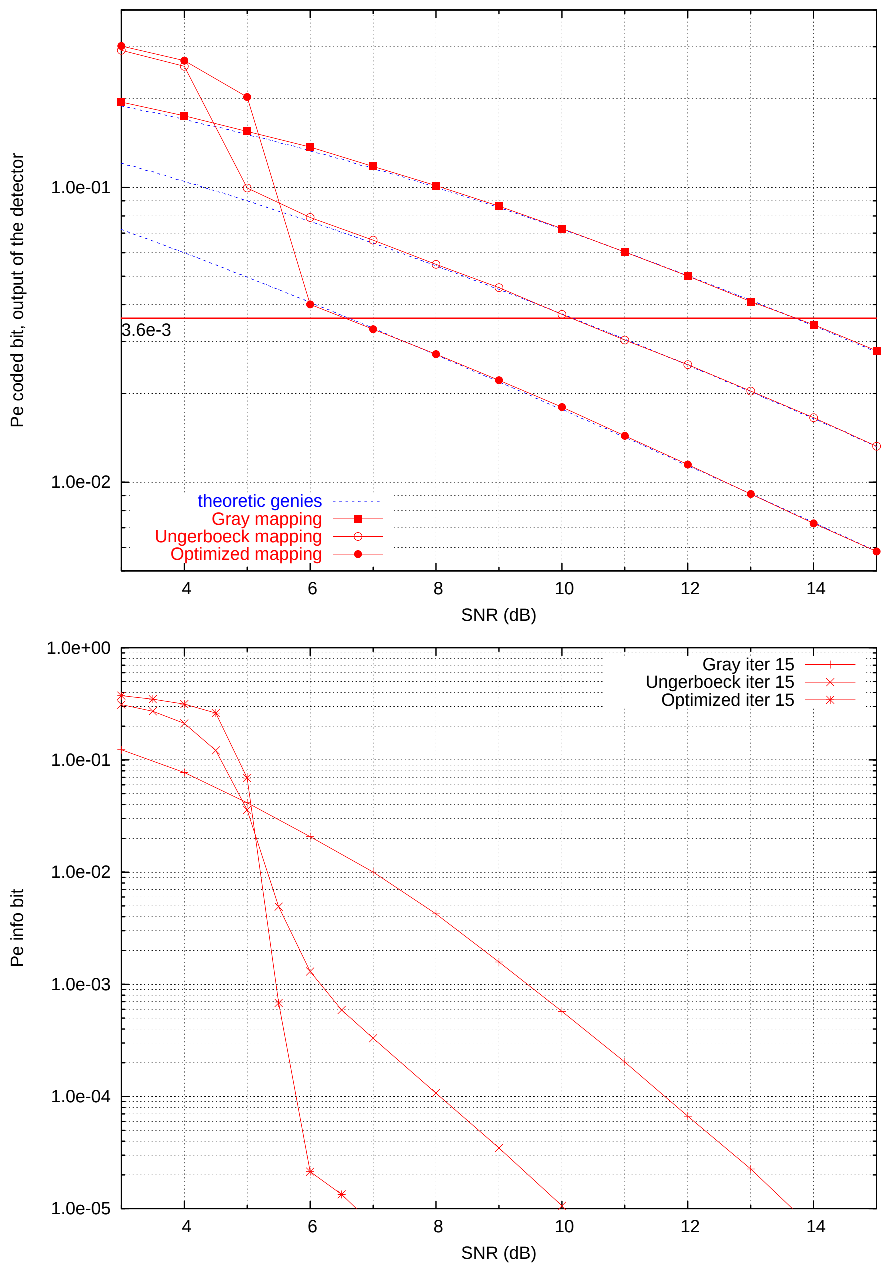

Figure 8: BER of a 4-state rate 1/2 convolutional code, at the input and output of the soft decoder (resp. upper and lower graphs), 16-QAM constellation, 1x1 Rayleigh fading channel.

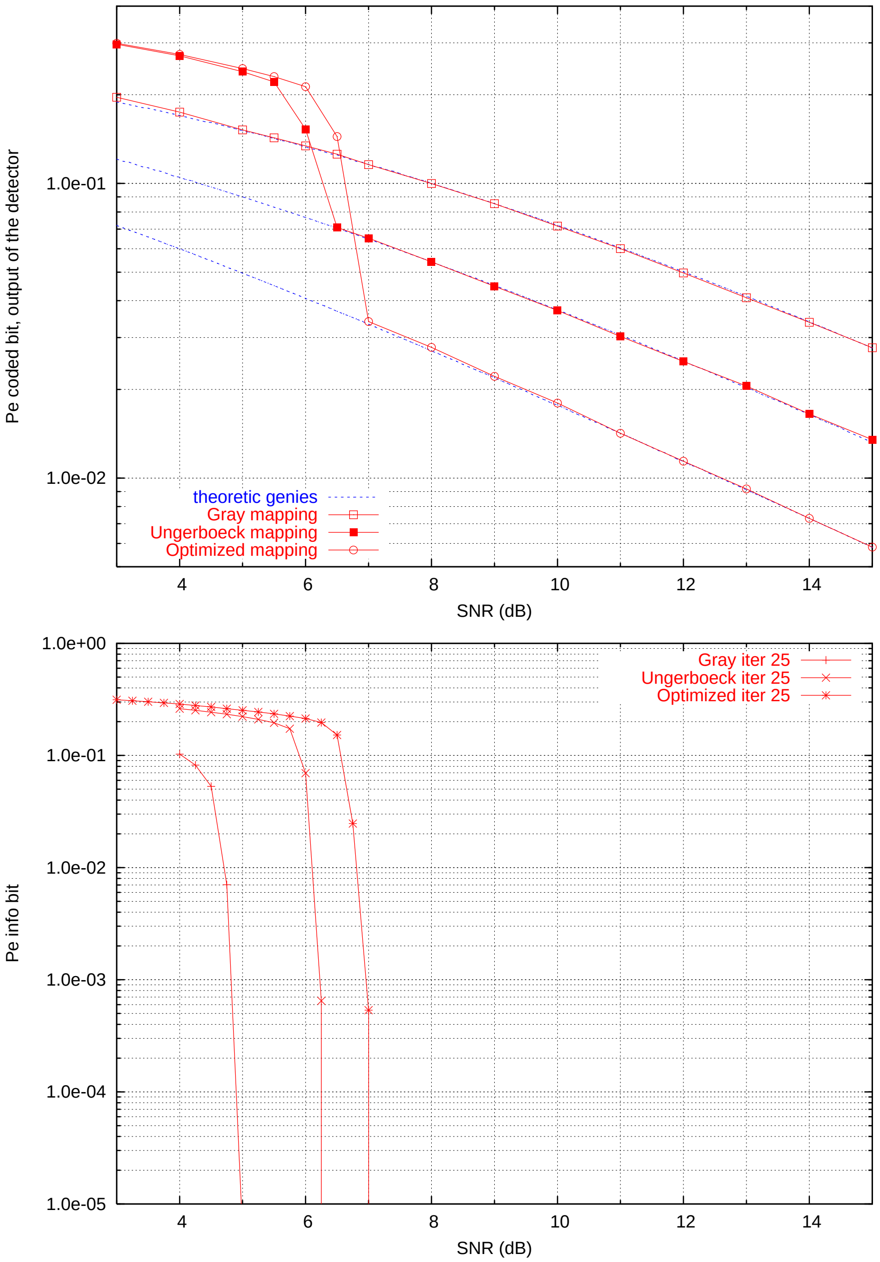

Figure 9: BER of a rate 1/2 parallel turbo code, at the input and output of the soft decoder (resp. upper and lower graphs), 16-QAM constellation, 1x1 Rayleigh fading channel.

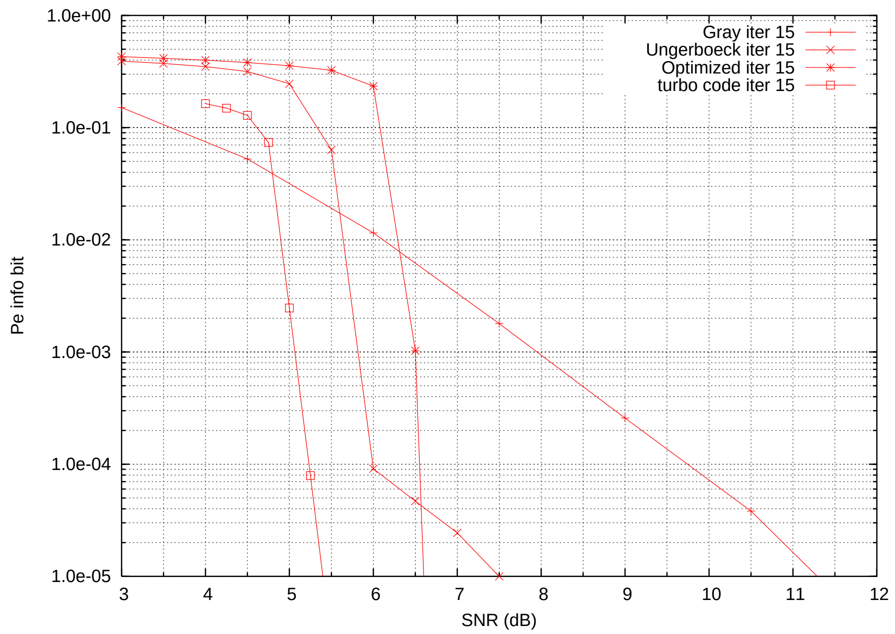

Figure 10: Performance of a 4-state rate 1/2 convolutional code versus turbo code, BER after decoding, 16-QAM constellation, 2x2 MIMO Rayleigh fading channel.

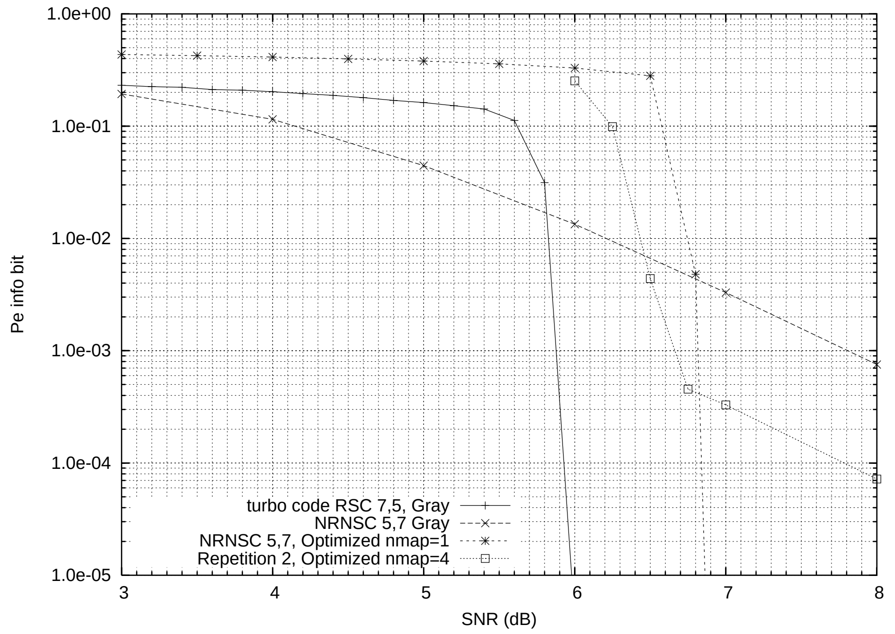

Figure 11: Performance of a 4-state rate 1/2 convolutional code versus turbo code and 1/2 repetition code with 8-dimensional mapping, BER after decoding, 16-QAM constellation, 4x4 MIMO Rayleigh fading channel.

4 Receiver study and design

4.1 Lattice representation of MIMO channels

Lattice theory [19] is a powerful mathematical tool to represent the channel geometrically and help us understand better its behavior in order to design a good modulator and its corresponding demodulator.
Since multi-dimensional QAM constellations are subsets of $\mathbb{Z}^n$, we can write $z \in \mathbb{Z}^{2n_t}$. Let n_s denote the dimension of the real Euclidean space,

$$n_s = 2 \times n_t = 2 \times n_r \tag{47}$$

The equality $x = zH$ is now extended to the real space $\mathbb{R}^{n_s}$ to get

$$x = zM, x \in \mathbb{R}^{n_s}, z \in \mathbb{Z}^{n_s} \tag{48}$$

Therefore, the MIMO channel output $y = x + \eta$ is obtained by perturbing a lattice point z with additive white noise η. A lattice Λ is a discrete subgroup of $\mathbb{R}^{n_s}$, i.e., it is a $\mathbb{Z}$-module of rank n_s. In (48), the lattice Λ is generated by the $n_s \times n_s$ real matrix M, which is derived from the channel matrix H by the following simple expression

$$M = \begin{pmatrix} \Re h_{11} & \Im h_{11} & \dots & \dots & \Re h_{1n_r} & \Im h_{1n_r} \\ -\Im h_{11} & \Re h_{11} & \dots & \dots & -\Im h_{1n_r} & \Re h_{1n_r} \\ \dots & \dots & \Re h_{ij} & \Im h_{ij} & \dots & \dots \\ \dots & \dots & -\Im h_{ij} & \Re h_{ij} & \dots & \dots \\ \Re h_{n_t1} & \Im h_{n_t1} & \dots & \dots & \Re h_{n_tn_r} & \Im h_{n_tn_r} \\ -\Im h_{n_t1} & \Re h_{n_t1} & \dots & \dots & -\Im h_{n_tn_r} & \Re h_{n_tn_r} \end{pmatrix} \tag{49}$$

The matrix M is called *lattice generator matrix*. Geometrically, the point x belongs to a discrete infinite set of points satisfying a group structure, i.e., a real lattice Λ. When z is restricted to a finite QAM integer constellation, then x belongs to a finite lattice constellation denoted by ζ. For example, if $n_t = n_r = 8$ antennas and $m = 4$ (16-QAM), the constellation ζ at the MIMO channel output has $2^{mn_t} = 2^{32} (\simeq 4)$ billion points ! Each point in ζ has a binary label of 32 bits. These bits are usually generated by an error correcting code such as a convolutional code or a turbo code.
Before combining an error-correcting code with a digital modulation for use on a MIMO channel, we first analyze the main parameters of the lattice Λ associated to multiple antenna channels. Such a geometrical analysis is complementary to the one made by information theory concerning Shannon capacity of MIMO channels.

Let P_Λ be the set of points that satisfies

$$P_\Lambda = \{x \in \mathbb{R}^n / x = \alpha M, \quad \alpha \in [0 \dots 1]^n\} \tag{50}$$

P_Λ is called the fundamental parallelotope of Λ (Figure 12).

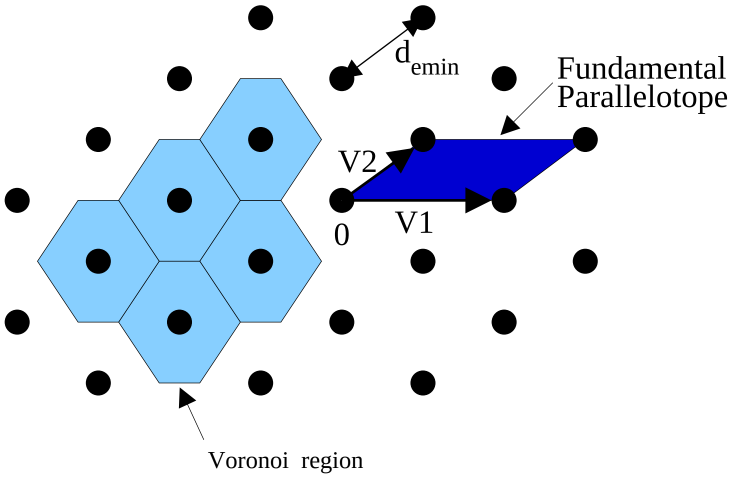

Figure 12: Lattice parameters

The first lattice parameter to be considered is the *fundamental volume* $vol(\Lambda)$, which represents the volume of the fundamental parallelotope defined by

$$vol(\Lambda) = |det(M)| = \sqrt{det(G)} \tag{51}$$

where the Gram matrix G defining the quadratic form $Q(z)$ associated to the lattice is related to M by

$$G = MM^t, ||x||^2 = zGz^t = Q(z) = \sum_{ij} g_{ij} z_i z_j \tag{52}$$

The second lattice parameter is the *minimum Euclidean distance* $d_{Emin}(\Lambda)$ defined by

$$d_{Emin}(\Lambda) = \min_{p1,p2} ||p_1 - p_2|| \quad p_1, p_2 \in \Lambda, p1 \neq p2 \tag{53}$$

The problem of computing $d_{Emin}(\Lambda)$ is hard (it is NP-complete). Thus, we suggest three different methods to get an estimation of the minimum Euclidean distance in Λ:

1. The lines of M are a $\mathbb{Z}$-basis for Λ. Read the n_s Euclidean norms in the lattice basis and keep the minimum. This yields an upper bound on $d_{Emin}(\Lambda)$. In practice, equivalently, we search for the minimum on the Gram matrix diagonal.

2. Reduce the basis M by finding another lattice basis with shorter vectors. We suggest here to use the efficient LLL reduction algorithm ([30]). This yields a tight upper bound on $d_{Emin}(\Lambda)$.

3. Find the exact minimum distance by enumerating lattice points inside a sphere centered on the origin, then take the minimal norm of a nonzero point. We suggest the application of *Short vectors* algorithm ([32]) to determine the exact value of $d_{Emin}(\Lambda)$.

Number of antennas	$d^2_{Emin}(exact)$ mean/variance	$d^2_{Emin}(LLL)$ mean/variance	$d^2_{Emin}(Gram)$ mean/variance	$\gamma(dB)$ mean/variance	$\gamma(dB) < 0$ Percentage
2	0.979/0.542	0.979/0.543	1.250/0.687	-1.10/2.04	78.1
4	1.607/0.576	1.608/0.579	2.182/0.803	-0.65/1.42	66.9
8	3.867/1.004	3.875/1.019	4.488/1.272	+0.76/0.75	17.1
16	9.719/2.231	9.734/2.274	9.770/2.309	+1.98/0.59	1.15

Table 2: Main lattice parameters of the MIMO channel (first table).

Number of antennas	$d^2_{Emin}(exact < LLL)$ Percentage	$d^2_{Emin}(LLL < Gram)$ Percentage	$d^2_{Emin}(exact < Gram)$ Percentage
2	0.19	40.02	40.07
4	0.92	61.60	61.86
8	3.18	53.82	54.67
16	2.36	4.79	5.64

Table 3: Main lattice parameters of the MIMO channel (second table).

Of course, the three methods above are listed in increasing order of complexity. As shown later in this study, the estimation of $d_{Emin}(\Lambda)$ helps to accelerate the Sphere Decoder algorithm ([45]) used to find the maximum likelihood (ML) lattice point.
Given the lattice minimum distance and its fundamental volume, it is possible to derive the normalized squared minimum distance, called *fundamental gain*, given by

$$\gamma(\Lambda) = \frac{d^2_{Emin}(\Lambda)}{vol(\Lambda)^{2/n_s}} \tag{54}$$

Usually, the fundamental gain is expressed in decibels, $\gamma_{dB} = 10log_{10}(\gamma)$. A lattice sphere packing is non-dense if $\gamma_{dB} < 0$, i.e., the lattice is less dense than the cubic integer lattice $\mathbb{Z}_s^n$. When $\gamma_{dB} > 0$, the dense lattice is associated to a *good* MIMO channel that may perform better than an AWGN single antenna channel. Such a performance comparison should also take into account the kissing number of Λ ([19]) which is completely random and difficult to estimate in a multiple antenna channel. Nevertheless, the three main parameters mentioned above are sufficient to understand the geometrical behavior of Λ. Tables 2 and 3 present the main parameters of a MIMO lattice and some statistics related to these parameters.

As expected, the lattice minimum distance increases with the number of antennas. Indeed, the channel diversity order is proportional to the number of antennas. The percentage of dense lattices is surprisingly high, especially for 8 and 16 antennas. This suggests a performance extremely close to the Gaussian channel when $n_t = n_r$ is large. If the channel matrix H is known by the transmitter, then it is possible to make a water-filling approach where the information instantaneous rate is proportional to $\gamma(\Lambda)$.

Two important results can be deduced from Table 3:

1. The LLL reduction algorithm is extremely efficient in finding the minimum distance of a MIMO lattice. The failure percentage varies from 0.19% to 3.18% only.

2. The simplest method (method 1 based on the diagonal of the Gram matrix) seems also quite efficient for a large number of antennas, (only 5.64% failure with 16 antennas).

Finally, Figures 13, 14, 15 and 16 give more details about the distribution of $d_{Emin}(\Lambda)$ and $\gamma(\Lambda)$ versus the number of antennas. Note that in Figure 16, in the case of 16 antennas, γ is limited to -1dB for non-dense lattices and upper bounded by 4dB for dense lattices. For comparison, we recall that $n_t = n_r = 16$ antennas correspond to a lattice in $\mathbb{R}^{32}$ for which some known structured dense lattices have a fundamental gain equal to 6dB.

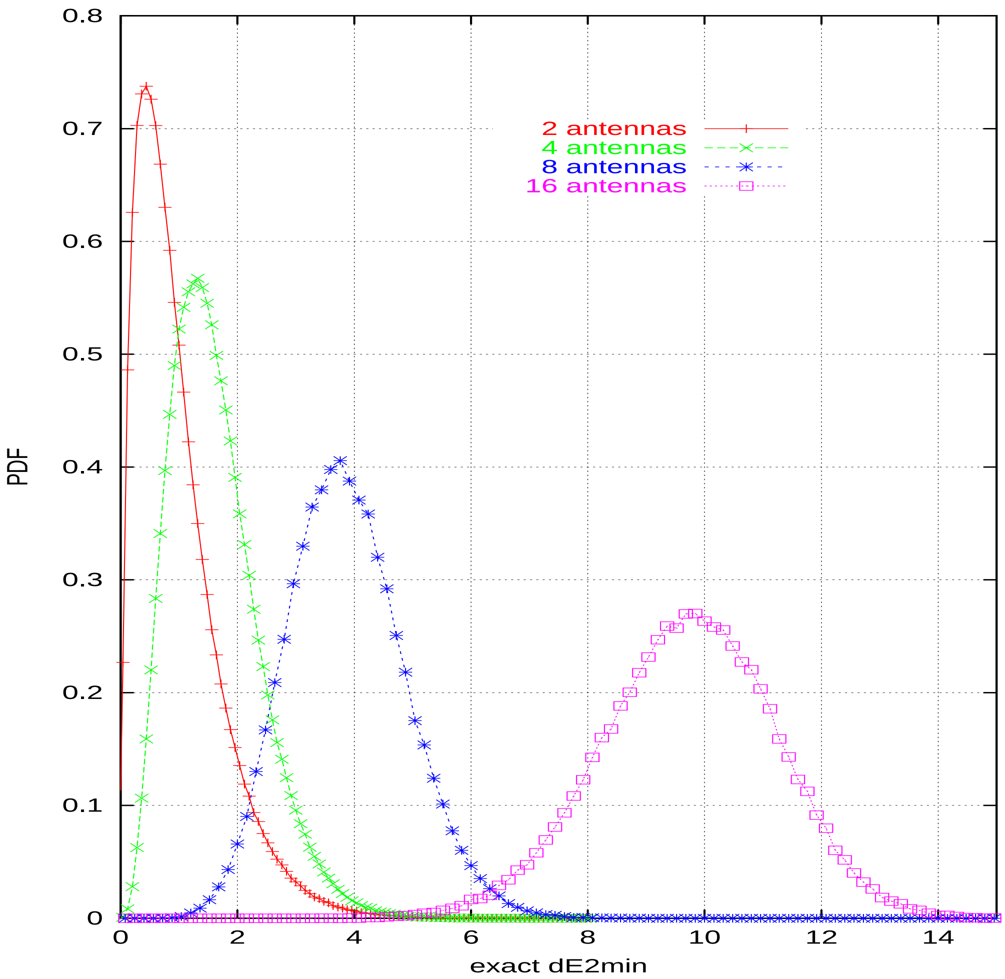

Figure 13: Distribution of the exact minimum squared distance d_{Emin}^2.

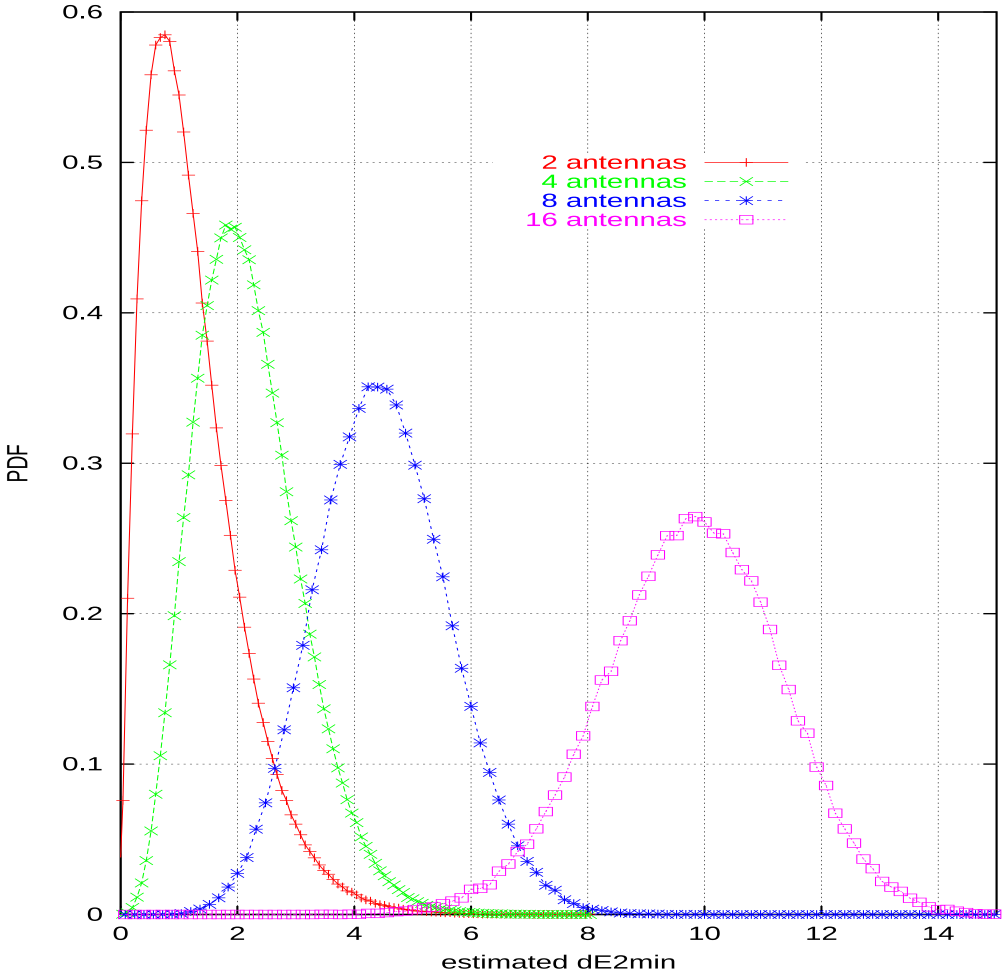

Figure 14: Distribution of d^2_{Emin} estimated from the Gram matrix.

4.2 Accelerated sphere decoding algorithm

A lattice point $x \in \Lambda(H)$ represents the signal received after a transmission over a MIMO channel. Here $\Lambda(H) = \Lambda(M)$ refers to the real lattice of rank n_s generated by M, or equivalently by H. A maximum likelihood lattice decoder applied to the received point $y = x + \eta$ determines the nearest lattice point to y, i.e., it minimizes $||y - x||$. A very efficient algorithm to find the closest point in a lattice when observing y is the sphere decoder [44, 45]. The main idea of this algorithm is to enumerate the points of the lattice that belong to a sphere centered on y and to calculate the distances between them. The point that minimizes the distance is called the closest point. If no point is found, the radius of the sphere have to be enlarged. Each time a point is found, the radius of the sphere can be reduced to the distance of this new point, which limits the number of points enumerated but still ensures the closest point criterion. The complexity of the sphere decoder depends on many points, as a non-exhaustive list, we cite the strategy of enumeration of the points

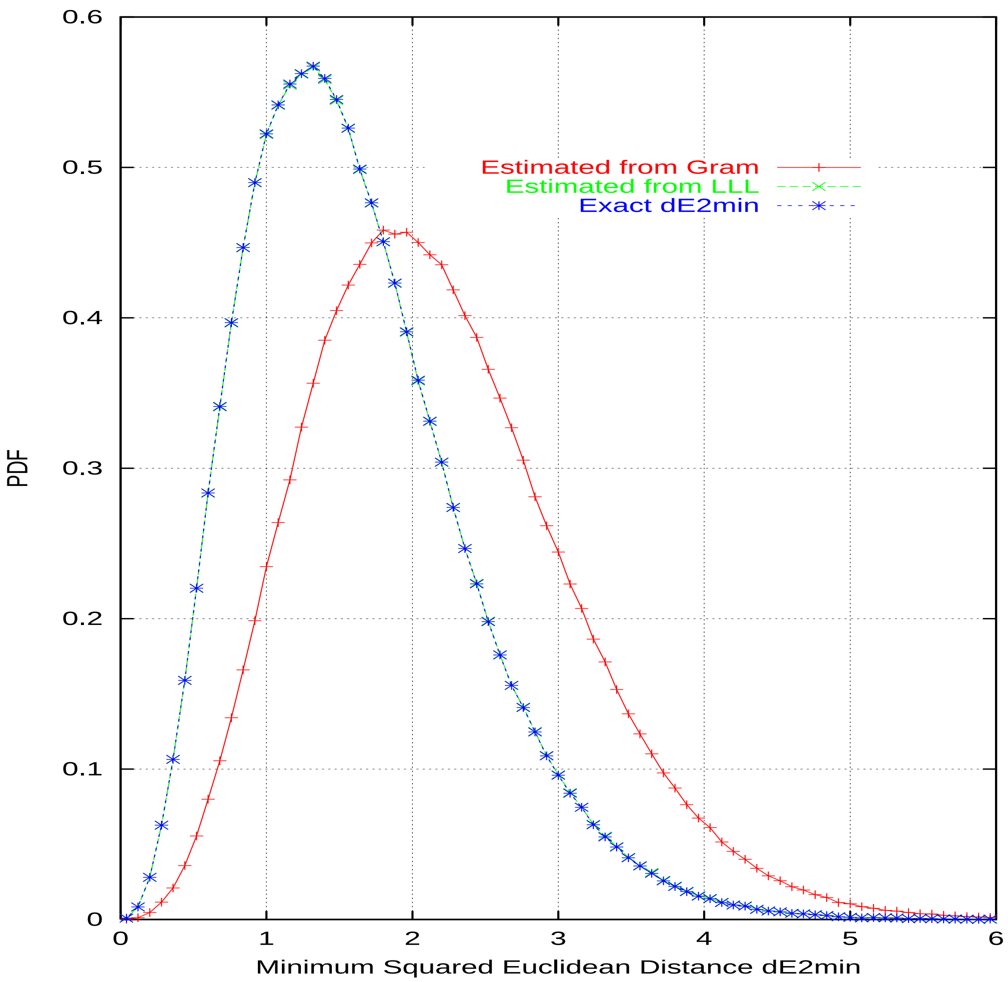

Figure 15: Comparison of different estimations of d^2_{Emin} for 4 antennas.

belonging to the sphere, the choice of the sphere radius and some complexity reductions that can be made in some particular cases, for example finite constellation. Two lattice decoding strategies are known in the literature :

- *The Sphere Decoder based on Pohst strategy*[32] was applied by Viterbo and Boutros (VB) [45] to digital communications. The key idea is to enumerate lattice points inside an ellipsoid in the integer space that corresponds to a spherical search region in the real space. The search complexity is sensitive to the choice of the initial radius.

- *The Sphere Decoder based on Schnorr-Euchner strategy*[35] was applied by Agrell, Eriksson,Vardy and Zeger (AEVZ) in [1]. The key idea is to view the lattice as laminated hyperplanes and then start the search for the closest point in the nearest hyperplane. A search radius can be specified in order to limit the search region to a sphere.

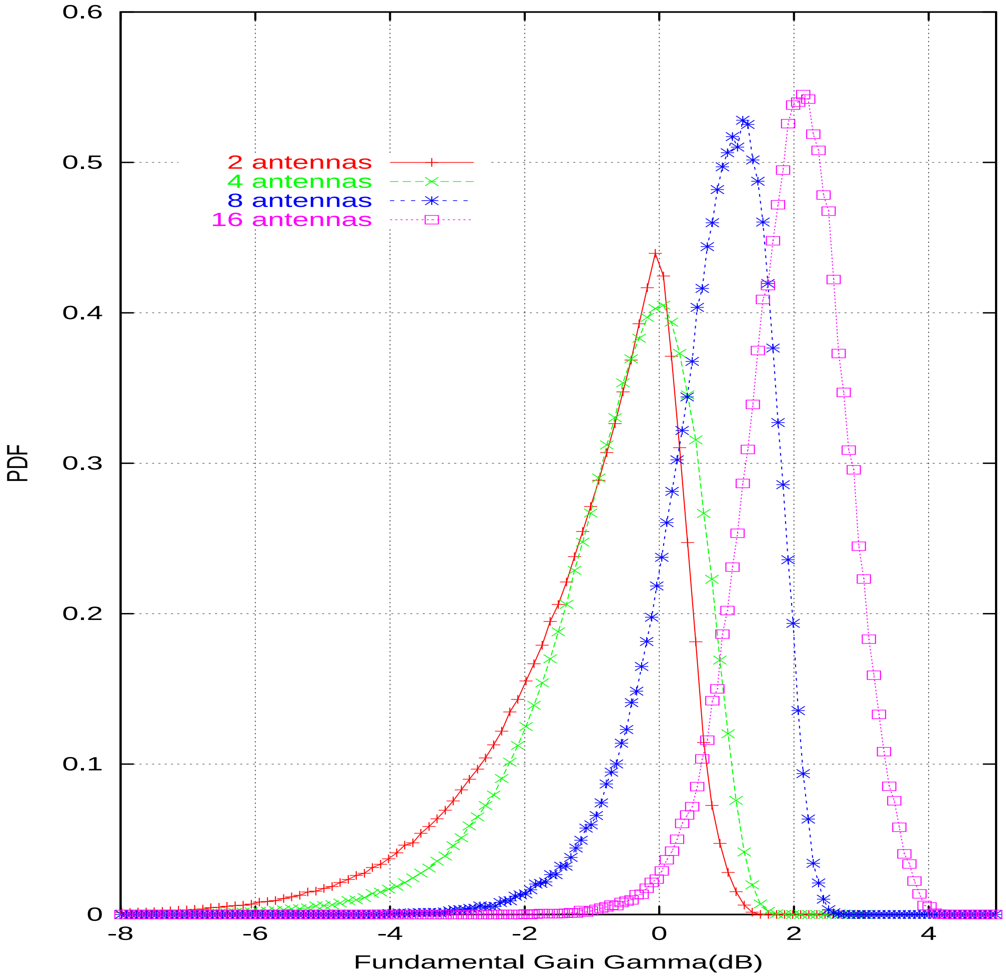

Figure 16: Distribution of the fundamental gain $\gamma(dB)$ in the MIMO channel.

The choice of the initial radius of the sphere is in general made by considerations on the noise or the lattice properties.
Recently, studies supported by computer simulations showed that AEVZ is two to four times faster than VB in finding the nearest point in a completely random lattice perturbed by uniformly distributed noise[1]. The factor 4 in speed ratio is measured after applying basis reduction like LLL (Lenstra-Lenstra-Lovasz [30]) or KZ (Korkine-Zolotareff [28]). For simplicity and in order to decode MIMO systems with a relatively large number of antennas (e.g., up to 16 transmit and 16 receive antennas), we exclude basis reductions from our study (even if the complexity of basis reduction is negligible if performed once in a frame as for block fading channels) because some complexity reductions, using the finite constellation properties, cannot be used with basis reduction.

A discrete subset ζ of Λ is called a constellation. For example, all the points $z \in \{\text{M-QAM}\}^n$ belong to a n-dimensional M-QAM [33] constellation of $\mathbb{Z}^n$. In digital communication finite systems which may be modeled by a lattice, the input of the channel z often belongs to a constellation in $\mathbb{Z}^n$ and thus, its noiseless output x belongs to a finite constellation in Λ. Finding the ML point is equivalent in finding the closest point in this constellation.

Based on the following arguments:

- In MIMO systems, the sphere decoder is used to decode a finite lattice constellation and not an infinite lattice. Implementing the constellation boundaries in the VB method, dramatically increases its speed compared to the AEVZ method.
- The lattice is perturbed by an additive gaussian noise and not an uniformly distributed noise. In the VB method, the initial search radius can be related to both the noise statistics and the lattice minimum distance in a way that drastically reduces its search complexity.

Hence, our accelerated sphere decoder is an AEVZ decoder that takes into account the QAM constellation boundaries by modifying the bounds of its internal counters, which have only been made for VB enumeration strategy. The algorithm of the sphere decoder with the Schnorr Euchner strategy and the modification of the bounds is presented below.

Also, our accelerated sphere decoder starts searching inside a radius judiciously chosen. Fig. 18 and Fig. 17 shows the bit error rate performance of the accelerated sphere decoder with up to 16 antennas and QPSK and 16-QAM, respectively. In the case of 16-QAM and 16×16 MIMO, the lattice constellation ζ has 2^{64} points. Even though, the accelerated sphere decoder succeeded relatively fastly in finding the ML point in the whole range $10^{-1}...10^{-6}$ of BER.

Sphere Decoder: Schnorr-Euchner strategy with bounds on the constellation: on next page.

Sphere Decoder: Schnorr-Euchner strategy with bounds on the constellation

Input. A received point y, the generator matrix $M(n \times n)$ of the lattice, the radius r of the sphere, and the bounds z_{min} and z_{max} of the constellation.

Output. The ML point z_{ML} belonging to the constellation and its distance to y

Step 1. (Pre-processing) Compute the Gram matrix $G = MM^T$ and the Cholesky's reduction $\{Q, R\} = Cholesky(G)$. R is upper-triangular. Compute $R^i = R^{-1}$ and $M^i = M^{-1}$

Step 2. (Initialization) Set $bestdist \leftarrow r^2$, $k \leftarrow n$, $dist_k \leftarrow 0$, $e_k \leftarrow yM^i$, $z_k \leftarrow [e_{kk}]$,$z_k \leftarrow max(z_k, z_{min})$,$z_k \leftarrow min(z_k, z_{max})$ compute $\rho = (e_{kk} - z_k)/(R^i_{kk})$, $step_k \leftarrow sign(\rho)$

Step 3. Compute $newdist \leftarrow dist_k + \rho^2$, if $newdist < bestdist$ and $k \neq 1$ then go to 4 else go to 5 endif

Step 4. compute for $i = 1, ..., k-1$ $e_{k-1,i} \leftarrow e_{k,i} - \rho R^i_{ki}$,decrease k, set $dist_k \leftarrow newdist$, $z_k \leftarrow [e_{kk}]$,$z_k \leftarrow max(z_k, z_{min})$,$z_k \leftarrow min(z_k, z_{max})$, $step_k \leftarrow sign(\rho)$ endif, go to 3

Step 5. if $newdist < bestdist$ then set $\hat{z} \leftarrow z$, $bestdist \leftarrow newdist$, else if $k = n$ then return $\hat{z}$ and terminate, else increase k, endif, compute $z_k \leftarrow z_k + step_k$,if $z_k < z_{min}$ or $z_k > z_{max}$ then $step_k \leftarrow -step_k - sign(step_k)$,$z_k \leftarrow z_k + step_k$ endif, if $z_k < z_{min}$ or $z_k > z_{max}$ then go to 5, endif, $\rho \leftarrow (e_{kk} - z_k)/R^i_{kk}$,$step_k \leftarrow -step_k - sign(step_k)$, go to 3

4.3 Soft output list decoding of a lattice constellation

Since there are n_t symbols emitted per channel use and m bits by symbol of the $2^m - QAM$, we have $m.n_t$ bits per channel use. Let c_j represent the j-th coded bit, $j = 0..m.n_t - 1$. Next we present how to find soft values for the coded bits from the observation y at the receive antenna array. The detector has two inputs: the received symbol y and the apriori probabilities on the coded bits $\pi(c_j)$. The two outputs of the detector are the a posteriori probabilities $APP(c_j)$ and the extrinsic probabilities $\xi(c_j)$ of the coded bits. We take for convention that the APP is the probability that the corresponding coded bit equals 1. Usually, to computes soft output, an exhaustive marginalization which take into account all the possible emitted symbols has to be processed. However, in this work, for complexity issues, this marginalization is limited to some points well chosen in a list.

4.3.1 Exhaustive APP detector

In this section, we present how to find soft values about the coded bits from the received signals based on the exhaustive list of the $2^{m.n_t}$ possible vectors $c^i = \{c^i_0, \dots c^i_{m.n_t-1}\}, i = 0..2^{m.n_t-1}$. We calculate the extrinsic probability $\xi(c_j)$ and a posteriori probability $APP(c_j)$ of each coded bit c_j, from the exhaustive list. The APP is equal to

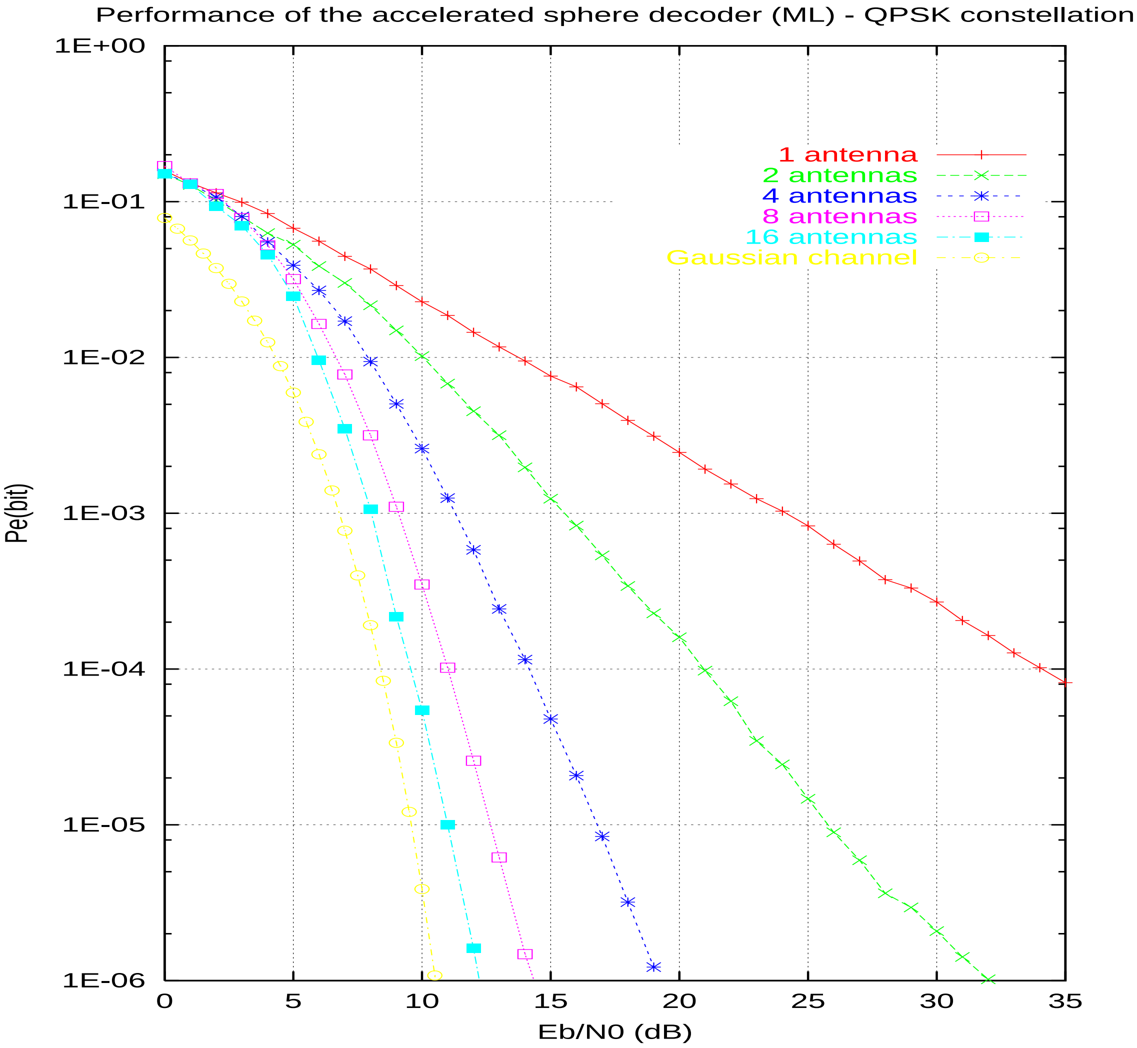

Figure 17: Bit error rate of a QPSK on a flat Rayleigh MIMO channel.

$$APP(c_j) = p(c_j|y) = \frac{p(y|c_j).\pi(c_j)}{p(y)} \quad \forall j = 0..m.n_t - 1 \tag{55}$$

where $\pi(c_j)$ is the a priori probability of the coded bit c_j. Moreover if we define the extrinsic probabilities at the output of the list by $\xi(c_j) = p(y|c_j)$, we have

$$APP(c_j) \propto \pi(c_j).\xi(c_j) \quad \forall j = 0..m.n_t - 1. \tag{56}$$

We can calculate the conditional probability $\xi(c_j) = p(y|c_j)$ by marginalizing the joint density of probability of the coded bits and the observation, with the hypothesis of mutual Independence of the received signal y_r given the coded bits c_j. We define

$$\Omega(c_j) = \{\tilde{c} : \tilde{c}_j = c_j, \quad \forall i \neq j, \tilde{c}_i \in \{0,1\}\} \tag{57}$$

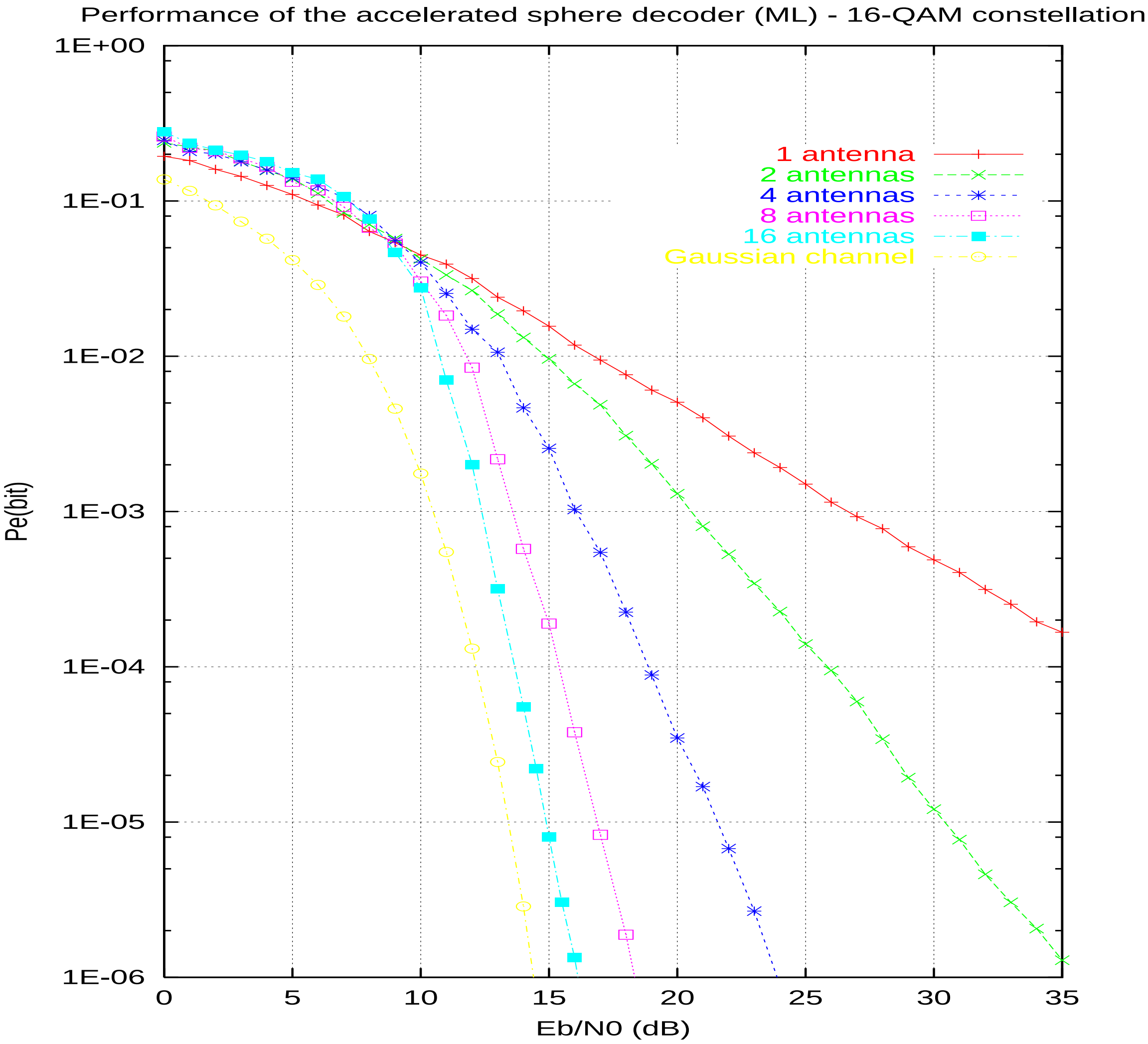

Figure 18: Bit error rate of a 16-QAM on a flat Rayleigh MIMO channel.

i.e. all the vectors of $\{0,1\}^{m.n_t}$ with their j-th bit fixed to the value c_j. The set Ω contains all possible emitted vectors which corresponds to the exhaustive list. To simplify the notations when we write $c \in \Omega$, we make reference to the vector of coded bits $\{c_0, \ldots, c_{m.n_t-1}\}$ and when we write $z \in \Omega$, we make reference to the vector of QAM symbols $\{z_0, \ldots, z_{n_t-1}\}$ corresponding to c.

Recall that $\xi(c_j) = p(y|c_j)$, so that:

$$\begin{aligned}
\xi(c_j) &= \sum_{\Omega(c_j)} p\left(y, c_0, \ldots, c_{j-1}, c_{j+1}, \ldots, c_{m.n_t-1} | c_j\right) \\
&= \sum_{\Omega(c_j)} p\left(y | c_0, \ldots, c_{m.n_t-1}\right) \prod_{r \neq j} \pi(c_r) \\
&= \sum_{\Omega(c_j)} \prod_{q=0}^{n_s-1} p\left(y_q | c_0, \ldots, c_{m.n_t-1}\right) \prod_{r \neq j} \pi(c_r).
\end{aligned}$$

Since the additive noise is white and Gaussian, we can express the conditional density of probability $p(y_q|c_0, \ldots, c_{m-1})$ by

$$p(y_q|c_0,\ldots,c_{m.n_t-1}) = \frac{1}{2\pi\sigma^2}e^{-\frac{\left\|y_q-\sum_{i=0}^{n_s-1} z_i m_{iq}\right\|^2}{2\sigma^2}} \tag{58}$$

$$p(y|c_0,\ldots,c_{m.n_t-1}) = \frac{1}{2\pi\sigma^2}e^{-\frac{\|y-zM\|^2}{2\sigma^2}} = \frac{1}{2\pi\sigma^2}\prod_{q=0}^{n_s} e^{-\frac{\left\|y_q-\sum_{i=0}^{n_s-1} z_i m_{iq}\right\|^2}{2\sigma^2}} \tag{59}$$

where the m_{ij}'s are the coefficients of the generator matrix M of the lattice and z the symbols emitted corresponding to the coded bits $\{c_0,\ldots,c_{m.n_t-1}\}$. To solve the problems of proportionality in (56), we normalize the extrinsic or APP probabilities to find the soft output of the decoder as

$$\xi(c_j) \leftarrow \frac{\xi(c_j=1)}{\xi(c_j=1)+\xi(c_j=0)} \tag{60}$$

Hence, the final equation is

$$\xi(c_j) = \frac{\sum_{z'\in\Omega(c_j=1)}\left[\left(e^{-\frac{\|y-z'M\|^2}{2\sigma^2}}\right)\prod_{r\neq j}\pi(c_r)\right]}{\sum_{z\in\Omega}\left[\left(e^{-\frac{\|y-zM\|^2}{2\sigma^2}}\right)\prod_{r\neq j}\pi(c_r)\right]} \tag{61}$$

4.3.2 Limitation of the likelihood

For systems whose equivalent lattice dimension is too important, the exhaustive marginalization becomes too complex. For example, a 2×2 MIMO requires a marginalization of 2^{16} points by channel use, and a 8×8 MIMO requires a marginalization of 2^{64} points by channel use. We propose to limit the marginalization to the points belonging to a list $\mathfrak{L}$. The approximated soft value becomes

$$\xi(c_j) = \frac{\sum_{z'\in\Omega(c_j=1)\cap\mathfrak{L}}\left[\left(e^{-\frac{\|y-z'M\|^2}{2\sigma^2}}\right)\prod_{r\neq j}\pi(c_r)\right]}{\sum_{z\in\Omega\cap\mathfrak{L}}\left[\left(e^{-\frac{\|y-zM\|^2}{2\sigma^2}}\right)\prod_{r\neq j}\pi(c_r)\right]} \tag{62}$$

We observe that the soft outputs depend both on the geometrical configuration when considering the likelihoods, and on the apriori probability configuration, which can be given by a decoder. In (61), some of the likelihoods are negligible. Let us suppose that all the points the likelihood of which is not negligible belong to a list $\mathfrak{L}$:

$$\forall z'\notin\mathfrak{L},\quad \forall z\in\mathfrak{L},\quad \frac{1}{2\pi\sigma^2}e^{-\frac{\|y-z'M\|^2}{2\sigma^2}} \ll \frac{1}{2\pi\sigma^2}e^{-\frac{\|y-zM\|^2}{2\sigma^2}} \tag{63}$$

The geometrical limit that separates these likelihoods is a sphere centered on the received point which justifies the construction of a non exhaustive list with the points of a sphere. The choice of the sphere radius determines the performance and the complexity of the corresponding soft-in soft-out detector and is the main difficulty of the solution presented by the authors. Indeed, the random nature of the channels implies a non stability in the list size. Another difficulty appears in the case of bursty channels, the list directly depends of the received point y, which necessitates the reconstruction of the list for each new received point, i.e., at each symbol time. Indeed, even if the channel is constant, the noise varies continuously, so do y.

4.3.3 A shifted spherical list

Once the ML point is found, and in the case of an ergodic channel, we choose to center the list on the ML point instead of centering it on the received point. Clearly, the marginalization (62) does not give the same results since the points in the list are different. We make the approximation that the output of the marginalization is quasi-equal to the output when the sphere is centered on the received point. Indeed, to compute efficient soft values, the radius of the sphere must be relatively high, and the points that will differ in the list are near the surface of the sphere, so they have the smallest likelihoods. In Fig. 19, we clearly see the advantages of the ML center when compared with the received point center. Indeed, when the received point is outside the constellation, which has a high probability when considering a large number of dimensions, the sphere centered on the received point enumerates a large number of lattice points to find a small number of constellation points. When the sphere is centered on the ML point, the number of listed points is reduced and the high likelihood points are taken into consideration.

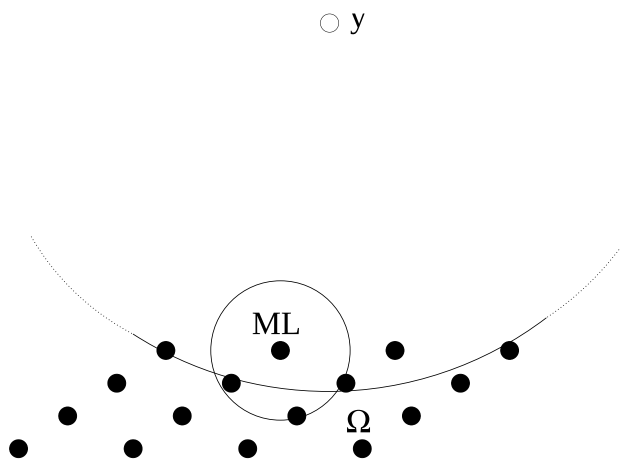

Figure 19: Comparison between the sphere centered on the ML point and the sphere centered on the received point y.

Since a classical SD finds in a lattice the closest point to a noisy received point, some changes have to be made to the SD algorithm to extend it to a soft-output sphere detector: the radius of the sphere is not reduced during the search like presented before, every point found in the intersection of the sphere and the constellation is stored, together with its distance to the received point. A double Pohst recursion is used to enumerate the points. Indeed, the first classical recursion is needed to check all lattice points at a squared distance less than the radius of the sphere centered on the ML point. We added a parallel second recursion to compute with a reduced complexity the distances between the enumerated points and the received point y (see step 3 in the description of the algorithm).

Spherical list enumeration

Input. A received point y, a point of the lattice x, the generator matrix $M(n \times n)$ of the lattice, the radius r of the sphere, and the bounds z_{min} and of the constellation.

Output. A list $\mathfrak{L}$ of points of the lattices that belong to the sphere, a list of the distance between y and each point of the list.

Step 1. (Pre-processing) Compute M^{-1}, $G = MM^T$ and the Cholesky's reduction $\{Q, R\} = Cholesky(G)$. R is upper-triangular. Compute $u = xM^{-1}$ and $\rho = yM^{-1}$.

Step 2. (Initialization) Set $d^2 \leftarrow r^2$, $T_n \leftarrow r^2$, $T_n^d \leftarrow r^2$. For $j = 1, .., n$ set $S_j \leftarrow u_j$, $S_j^d \leftarrow \rho_j$, $i \leftarrow n$ and $u \leftarrow 0$

Step 3. Compute $L_{inf} \leftarrow max\left(\left\lfloor\sqrt{T_i/q_{ii}} + S_i\right\rfloor, z_{min}\right)$ and $z_i \leftarrow min\left(\left\lceil-\sqrt{T_i/q_{ii}} + S_i\right\rceil, z_{max}\right) - 1$

Step 4. Increase z_i, If $z_i > L_i$ if $i > 1$ compute $\xi_i \leftarrow u_i - z_i$ and $\xi_i^d \leftarrow \rho_i - z_i$, compute $T_{i-1} \leftarrow T_i - q_{ii}(S_i - z_i)^2$ and $T_{i-1}^d \leftarrow T_i^d - q_{ii}(S_i^d - z_i)^2$,compute $S_{i-1} \leftarrow u_{i-1} + \sum_{j=1}^n q_{i-1,j}\xi_j$ and $S_{i-1}^d \leftarrow \rho_{i-1} + \sum_{j=1}^n q_{i-1,j}\xi_j^d$, decrease i and go to Step 4, endif, else compute $\hat{d}^2 \leftarrow r^2 - T_i^d + q_{11}(S_1^d - z_1)^2$, store z and $\hat{d}$ in $\mathfrak{L}$, increase u and go to Step 4, endif, endif , else if $i = n$ terminate else increase i and go to Step 4, endif, endif

Instead of centering the sphere on the ML point, we can evaluate it with classical sub-optimal methods to reduce the complexity of the system. As a non exhaustive list, we cite some known methods that can be implemented as an alternative to the sphere decoder:

- Zero Forcing (ZF) with or without a hard decision.
- Minimum Mean Square Equalizer (MMSE) with or without a hard decision.
- Interference Cancellation with or without ordering (MMSE or ZF).

Until the end of this document, we only discuss the case when the sphere is centered on the ML point, the above simplifications can be applied in most of the cases.

4.3.4 Choice of the radius

The choice of the sphere radius R for this list sphere decoder is as important as the choice of the radius for the conventional SD. Having too many points in the sphere heavily slows down the detection while not having enough points degrades significantly the performance. In this section, some properties of lattices are exploited to determine a sphere radius that guaranties a stability in the number of points in the list. Let us assume we want to find N_p points to create a list centered on the origin 0. We make the approximation that the volume of a sphere containing N_p points is equal to the volume of N_p fundamental parallelotopes. Hence, the radius R of a sphere that contains about N_p points is well approximated by

$$R = \left(\frac{N_p \times vol(\Lambda)}{V_n}\right)^{\frac{1}{n}} \tag{64}$$

where $vol\,(\Lambda)$ is the fundamental volume of the lattice and V_n is the volume of a unitary sphere in dimension n:

$$V_n = \frac{\pi^{n/2}}{\Gamma(n/2+1)} = \begin{cases} \frac{\pi^{n/2}}{(n/2)!} & n \text{ pair} \\ \frac{2^n \pi^{(n-1)/2}((n-1)/2)!}{n!} & n \text{ impair} \end{cases} \tag{65}$$

This method of choosing the radius is quite stable in a lattice when N_p is high. When considering a constellation, the intersection between the sphere and the constellation significantly diminishes the number of selected points. Depending on the position of the ML point in the constellation, the number of enumerated points varies. Fig. 20 shows a situation where 13 points are enumerated in the lattice and only 7 points in the constellation.

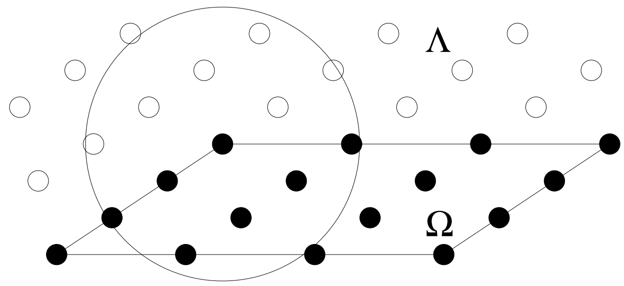

Figure 20: The loss of points in the list in the case of constellations

We can adjust the sphere radius taking into account the number of hyperplanes n_{hyp} the ML point belongs to. The number of expected points N_p is multiplied by $\alpha[n_{hyp}]$, an expansion factor of the list size which depends on n_{hyp}. Indeed, the more the number of hyperplanes the ML point belongs to, the less the points in the list. For example, the choice $\alpha[i] = \lfloor i/2 \rfloor + 1$ gives good results.
The number of listed points is also influenced by the lattice geometry. The more dense the

lattice, the more stable the list. Indeed, the side effects are less important. To take into account this property, we could use the fundamental volume $\gamma(\Lambda)$ and add a pre-correction of the expected number of points to the list radius. The problem of finding d^2_{Emin} is NP complex, that is why we approximate it by the minimum of the diagonal of the Gram matrix. We will call $g^2_{min}(\Lambda)$ this quantity and γ_G the approximation of the fundamental gain of Λ:

$$\gamma_G(\Lambda) = \frac{g^2_{min}(\Lambda)}{|det(M)|^{2/n_s}} \tag{66}$$

We then use a simple criterion for an additional expansion μ of the number of points:

$$\begin{cases} \gamma_G(\Lambda)dB > \gamma_1 \Rightarrow \mu_\gamma = \mu_1 \\ \gamma_G(\Lambda)dB > \gamma_2 \Rightarrow \mu_\gamma = \mu_2 \end{cases} \tag{67}$$

E.g., we take $\gamma_1 = 3dB, \gamma_2 = 6dB, \mu_1 = 4, \mu_2 = 16$.

Finally, the new radius is given by

$$R = \left(\frac{\alpha[n_{hyp}] \times \mu_\gamma \times N_p \times det\,(G)}{V_n} \right)^{\frac{1}{n}} \tag{68}$$

If the number of points in the list is too small, we can reenumerate the points in a larger sphere, for example by multiplying the radius by 1.5.

4.3.5 Complexity reduction for block fading channels

Let us define N_{block} the number of symbols in a code word. In the case of an ergodic channel, we have to store N_{block} lists to calculate the observations on all coded bits before giving them to the observation input of the SISO decoder. In the case of a block fading channel, the channel remains unchanged during the block. Thanks to the lattice structure, we can find the points in the sphere centered on the origin of the lattice and translate them to find the points in the sphere centered on x_{ML}. This invokes the translation invariance of the lattice (cf Fig. 21).

In the list, we store $n_{\mathfrak{L}}$ points belonging to the constellation with their labeling. For each channel use, the noise changes, so the distances to the received point have to be reprocessed. A less efficient version only takes into account the distance to the ML point, so the distances are processed once at the beginning of each block.

We can also enumerate a larger list and sort it with the distance to the origin. This can be seen as a list of concentric spheres. If the first sphere leads to a list which is too small, we consider the second sphere and so on (see Fig. 22).

4.3.6 Applications to iterative detection and decoding of BICM

In this section, we illustrate the application of the new soft detector to BICM on MIMO. The symbols z_i belongs to an M-QAM constellation. The transmitter structure is illus-

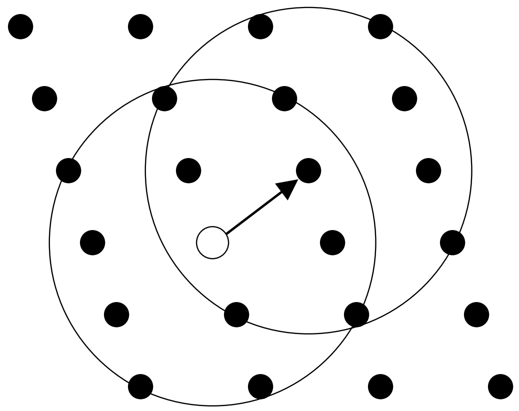

Figure 21: Translation invariance of the lattice

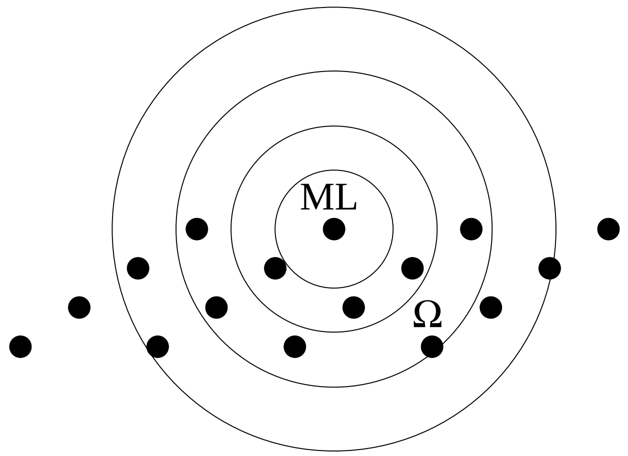

Figure 22: A concentric list of spheres

trated in Fig. 23. The information binary elements are encoded by a rate R_c convolutional code. The coded bits $\{c_\ell\}$ are randomly interleaved and fed to a QAM mapper ($M = 2^m$) that generates z. The spectral efficiency of the system is $R_c \times m \times n_t$ bits per channel use, or equivalently, $R_c \times m \times n_t$ bits/sec/Hz. An iterative joint detection and decoding receiver is based on the exchange of soft values between the SISO QAM-detector and the SISO code decoder. The SISO detector computes the extrinsic probabilities $\xi(c_\ell)$ via the classical sum product expression (62) including the conditional likelihoods $p(y/z)$ and the a priori probabilities $\pi(c_\ell)$ fed back from the SISO decoder. By exploiting the trellis structure of the code, the SISO decoder computes the soft values (a posteriori probabilities and extrinsics) for the coded bits using the Forward-Backward algorithm [3]. The information exchange between inputs and outputs of the two blocks is shown on Fig. 4.3.6.

When there is only one symbol representing one bit in the list, the observation is either 1 or 0. In that case there is no point in the constellation with the other symbol, which can cause calculus inconsistency when marginalizing. For example, in Fig. 25, if we consider that the a priori of the first bit is equal to 0.0, the SISO decoder fails because there is no

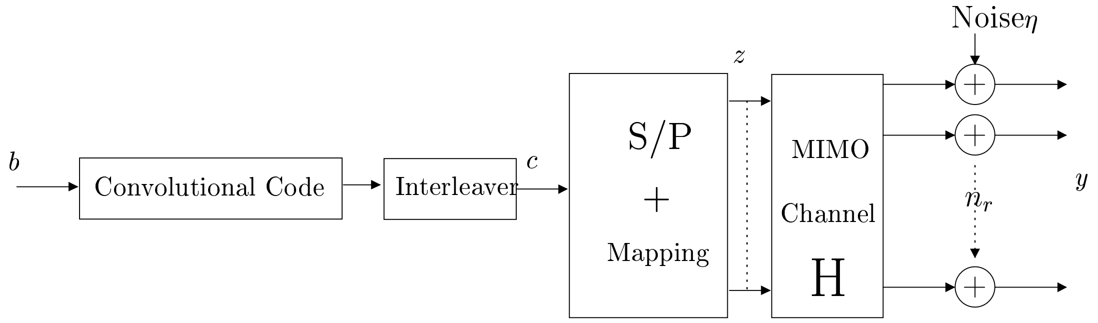

Figure 23: System model

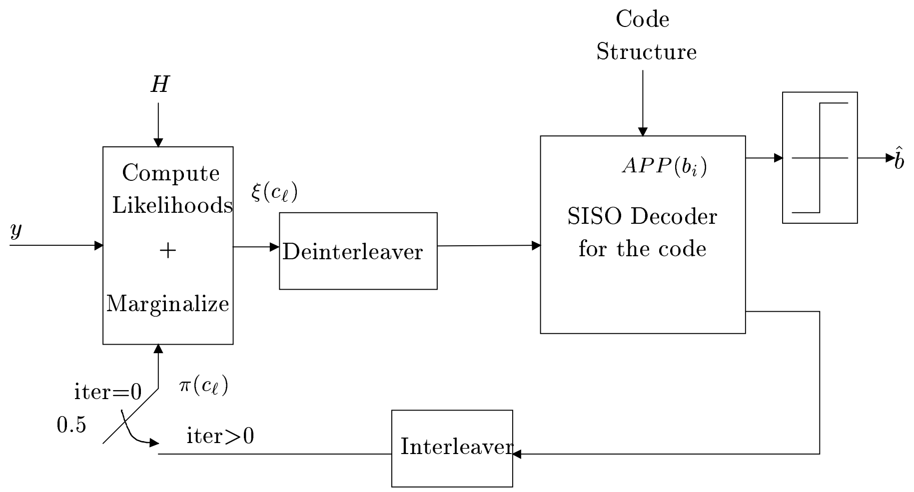

Figure 24: Exhaustive List Decoder

point corresponding to a first bit equal to 0 in the list. Without loss of generality, we will consider this case until the end of this section.

A first solution to solve the inconsistency problem is to replace the APP of the considered bit by the minimum among the contributions in the list, (62) becomes

$$\tilde{\xi}(c_j) = \left[1 + \frac{\min_{z' \in \Omega(c_j=1) \cap \mathfrak{L}} \left(\left(e^{-\frac{\|y-z'M\|^2}{2\sigma^2}} \right) \prod_{r \neq j} \pi(c_r) \right)}{\sum_{z' \in \Omega(c_j=1) \cap \mathfrak{L}} \left[\left(e^{-\frac{\|y-z'M\|^2}{2\sigma^2}} \right) \prod_{r \neq j} \pi(c_r) \right]} \right]^{-1} \tag{69}$$

Another solution is to consider the worst case when the nearest point with the considered bit equal to 0 is at the surface of the sphere. In this case, we consider the sphere radius to calculate its likelihood. The corresponding apriori probability π_v of this virtual point can be chosen in different ways:

- By an average case when all apriori probabilities equal 0.5:

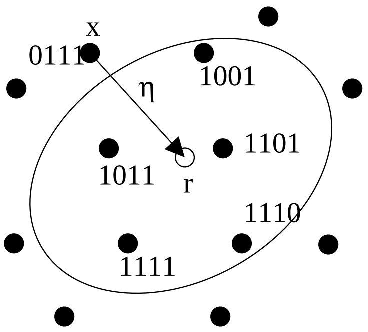

Figure 25: Situation leading to inconsistency

$$\pi_v = 0.5^{m.n_t-1} \tag{70}$$

- By the worst case when the point is of higher a priori probability:

$$\pi_v = \prod_{r\neq j} \max\left\{\pi(c_r), 1-\pi(c_r)\right\} \tag{71}$$

With this method, (62) becomes

$$\tilde{\xi}(c_j) = \left[1 + \frac{\pi_v.e^{-\frac{R^2}{2\sigma^2}}}{\sum_{z'\in\Omega(c_j=1)\cap\mathfrak{L}}\left[\left(e^{-\frac{\|y-z'M\|^2}{2\sigma^2}}\right)\prod_{r\neq j}\pi(c_r)\right]}\right]^{-1} \tag{72}$$

Another efficient way to reduce inconsistency calculus problems is to apply a ceiling on the soft values exchanged between the blocks. A first ceil with parameter ϵ_c is applied to soft values given by the soft decoder to the detector, i.e., a priori probabilities for the detector:

$$\forall j, \quad \begin{cases} \pi(c_j) < \epsilon_c \Rightarrow \pi(c_j) \leftarrow \epsilon_c \\ \pi(c_j) > 1-\epsilon_c \Rightarrow \pi(c_j) \leftarrow 1-\epsilon_c \end{cases} \tag{73}$$

The same method can be applied at the output of the detector with parameter ϵ_l, but it is preferable to apply the ceiling during the computation of the a priori probabilities product

Initialization $\alpha_j \leftarrow 1-\epsilon_l$
for $r=0$ to $m\times n_t$ and $r\neq j$, $\alpha_j \leftarrow \alpha_j \times \pi(c_r)$,$\alpha_j \leftarrow \max\left\{\alpha_j, \epsilon_l\right\}$

Indeed, we can see that the perfect, but problematic, case when $\alpha_j = 1$ is solved by initializing α_j to $1-\epsilon_l$. During the computation, if the current product becomes inferior

to ϵ_l, a ceiling is done, which limits the calculation distortion.
At the end of the computation, α_j gives an estimation of the product of the a priori probabilities in the computation (72). The parameters ϵ_l and ϵ_c can for example be chosen equal to 10^{-5}.

4.4 Applications of the spherical list to MIMO channel mutual information computation

4.4.1 MIMO Mutual information computation

The capacity C of a channel and its mutual information $I(z;y)$ between its input z and output y are two essential quantities that are necessary to compute when designing optimal performance systems. Indeed, for a given coding Rate R_c, they give a lower bounds on the signal to noise ratio E_b/N_0. The capacity C of a MIMO channel has been established in ([41]), z is a complex gaussian entries vector:

$$C = E_H\left\{log_2\left(det\left(I + \frac{H.R_{zz}.H^H}{N_0}\right)\right)\right\} \tag{74}$$

The mutual information between the constellation point z and the output symbol of the channel y is given by

$$I(z;y) = m.n_t - \frac{1}{2^{m.n_t}}\sum_z \int_y p(y/z)log_2\left(\frac{\sum_{z'} p(y/z')}{p(y/z)}\right)dy \tag{75}$$

This quantity can be computed, like (74), by a Monte-Carlo simulation:

$$I(z;y) = m.n_t - E_{z,H,\eta}\left\{log_2\left(\frac{\sum_{x'} p(y/z')}{p(y/z)}\right)\right\} \tag{76}$$

We have the choice to make the expectation over z, H and η separately or jointly. The best results will be given by the first expectation but will need longer time. We will take into account here some symmetries of the channel that permits to limit the complexity of the first expectation process.

Let us define:

$$f(z,H) = -\int_y \sum_z p(y/z)p(z)log_2\left(\frac{\sum_{z'} p(y/z')p(z')}{p(y/z)}\right)dy \tag{77}$$

The average mutual information (we suppose a non-stationnary channel) is given by

$$I(Z;Y) = E_{H,z,\eta}\left(I_H(Z=z;Y=y)\right) = \int_H p(H)\sum_z f(z,H)dH \tag{78}$$

The evaluation of this mutual information with a separated expectation Monte-Carlo method is prohibitive when we consider more than 2 antennas in emission and reception and a 16-QAM modulation (this expectation needs $2^{m.n_t} \times N_H \times N_\eta$ random samples where N_H is the number of samples for the channel and N_η is the number of samples for the noise). We can use a property of the channel to simplify the evaluation of this mean. Indeed, the phase of each entry of a MIMO channel is uniformly distributed. We consider two points z and z' that only differ with their phase :

$$z' = \{z'_0 = z_0 e^{j\phi_0}, \dots z'_{n_t} = z_{n_t} e^{j\phi_{n_t}}\} = \phi z \tag{79}$$

Where the matrix ϕ is diagonal defined by

$$\phi = diag\{e^{j\phi_i}\} \tag{80}$$

The phase of each entries of the matrix H is uniformly distributed, so $p(H(\rho, \phi)) = p(H(\rho))$:

$$\int_H p(H) f(z, H) dH = \int_\rho \int_\phi p(H(\rho)) f(z, H(\rho, \phi)) d\phi d\rho \tag{81}$$

$$f(z', H(\rho, \phi)) = f(z, H(\rho, \phi')) \tag{82}$$

$$\Rightarrow \int_H p(H) f(z, H) dH = \int_H p(H) f(z', H) dH \tag{83}$$

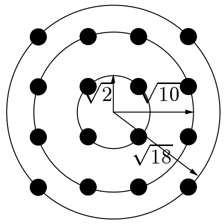

Figure 26: Modulos of a 16QAM constellation

We can replace all the points that have the same module configuration by a single "virtual point", for example on Fig. 26 we can see that only 3 "virtual points" have to be taken into account in the sum over z. The point of modulo $\sqrt{2}$ have a weight equal to 4, the point of modulo $\sqrt{10}$ has a weight equal to 8 and the point of modulo $\sqrt{18}$ has a weight equal to 4.

We consider the weights $N_p(z)$ to be the number of points that have the same module configuration than z. For example, when we consider 2 antennas in emission with a 16-QAM constellation, we only have to consider 3^2 points instead of 16^2. Let Ω be the set of points that are sufficient to calculate the mutual information, $\Omega \in \Lambda$, where Λ is the constellation.

The mutual information is now given by

$$I(Z;Y) = log_2 2^{m.n_t} - \frac{1}{2^{m.n_t}} \int_H \int_y \sum_{z\in\Omega} N_p(z) p(y/z) log_2 \left(\frac{\sum_{z'} p(y/z')}{p(y/z)} \right) dydH \tag{84}$$

We can estimate this mutual information with a Monte-Carlo simulation, with N_n realizations of the noise, N_H realizations of the channel.

$$\widetilde{I(Z;Y)} = m.n_t - \frac{1}{2^{m.n_t} \times N_n \times N_H} \sum_{H}^{N_H} \sum_{z\in\Omega} N_p(z) \sum_{b}^{N_n} log_2 \left(\frac{\sum_{z'\in\Omega} e^{-\|y-z'H\|^2/2N_0}}{e^{-\|y-zH\|^2/2N_0}} \right) \tag{85}$$

Nonetheless, the numerator of the logarithm is computed by an exhaustive marginalization of the $2^{m.n_t}$ symbols z' of the constellation Ω, which limit simulations to $m.n_t \leq 8$ (for example 16-QAM on MIMO 4x4 is unfeasible).

4.4.2 Bounds with the spherical list

We can limit the complexity of the marginalization only taking into account the points in a well chosen subset of the constellation, for example the spherical list $\mathfrak{L}$ of radius R centered on the received point described before. Each point z' at the outside of the sphere has its likelihood upper bounded by the likelihood $p(y/z_s)$ of a point z_s lying at the surface of the sphere:

$$p(y/z_s) = \frac{exp\left(-R^2/2N_0\right)}{\sqrt{2\pi N_0}} \tag{86}$$

There are $(|\Omega| - |\mathfrak{L}|)$ points that do not belong to the list $\mathfrak{L}$, where $|\Omega|$ and $|\mathfrak{L}|$ represent the cardinals of Ω and $\mathfrak{L}$, respectively. We can express upper and lower bounds to the numerator of the logarithm in (75):

$$\sum_{z\in\mathfrak{L}} p(y/z) \leq \sum_{z\in\Omega} p(y/z) \leq \sum_{z\in\mathfrak{L}} p(y/z) + (|\Omega| - |\mathfrak{L}|)\,.p(y/z_s) \tag{87}$$

This leads to upper and lower bounds to $I(z;y)$:

$$\begin{cases} I(z;y) \geq m.n_t - E_{z,H,\eta}\left\{ log_2 \left(\frac{\sum_{z'\in\mathfrak{L}} p(y/z') + (|\Omega|-|\mathfrak{L}|).p(y/z_s)}{p(y/z)} \right) \right\} \\ I(z;y) \leq m.n_t - E_{z,H,\eta}\left\{ log_2 \left(\frac{\sum_{z'\in\mathfrak{L}} p(y/z')}{p(y/z)} \right) \right\} \end{cases} \tag{88}$$

We have already seen in the list detector section that the list centered on the received point y is not as controllable as the list on the ML point. Indeed, the radius of the sphere can be corrected before the enumeration of the points depending on the situation of the ML point in the constellation. Nevertheless, we do not have again an upper bound on the mutual information $I(z;y)$ when considering the substitution of the likelihoods of the missing points by the likelihood $p(y/z_s)$. For example, in Fig. 27, we can see that the

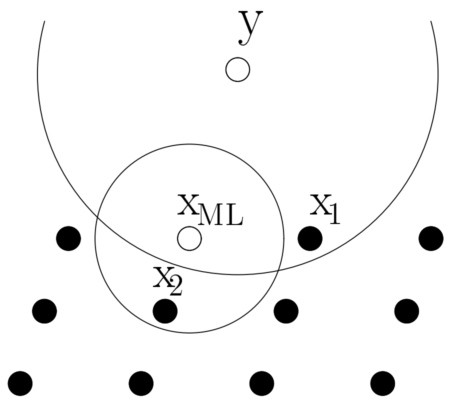

Figure 27: Illustration on how to approximate $I(x;y)$

x_2 point's likelihood is lower than the x_1 point's one, the likelihood of the missing points cannot be upper bounded.

An other important quantity that can be used in BICM is the mutual information between the ith coded bit c_i and the received symbol y. This mutual information is calculated from the equation

$$I(c_i;y) = 1 - E_{z,H,\eta}\left\{log_2\left(1 + \frac{\sum_{z'\in\Omega(\overline{c}_i)} p(y/z')}{\sum_{z''\in\Omega(c_i)} p(y/z'')}\right)\right\} \tag{89}$$

Where $\Omega(c_i)$ represents the subset of points of the constellation which ith bit is equal to c_i. Again, we can use a spherical list to limit the complexity and derivate the bounds (87) to calculate the upper and lower bounds of $I(c_i,y)$ when $\mathfrak{L}$ is centered on the received point y:

$$\left\{\begin{array}{l} I(z;y) \geq 1 - E_{z,H,\eta}\left\{log_2\left(\frac{\sum_{z'\in\mathfrak{L}(\overline{c}_i)} p(y/z') + (|\Omega| - |\mathfrak{L}(\overline{c}_i)|).p(y/z_s)}{\sum_{z'\in\mathfrak{L}(\mathfrak{c}_i)} p(y/z')}\right)\right\} \\ I(z;y) \leq 1 - E_{z,H,\eta}\left\{log_2\left(\frac{\sum_{z'\in\mathfrak{L}(\overline{c}_i)} p(y/z')}{\sum_{z'\in\mathfrak{L}(\mathfrak{c}_i)} p(y/z') + \left(|\Omega| - |\mathfrak{L}(\mathfrak{c}_i)|\right).p(y/z_s)}\right)\right\} \end{array}\right. \tag{90}$$

4.5 Computer simulations and numerical results

We can use any existing code but the more complex to interface with the detector are concatenated codes because of the iterative processing in the decoding procedure. We have chosen to present turbo-codes, the use of other types of error-correcting codes is straightforward. Let us consider a rate $R = k/n = 1/2$ turbo code whose constituent codes are two $(1, 5/7)$ RSC convolutional codes. The output of each code is punctured by a factor 2. This encoding is depicted on Fig. 28. We define $L = 3$ the constraint length of the constituent codes. The information bits are grouped into blocks of length $R.m.T_{coh}$ where $k = 1$. The tail bits of the two RSCs are not punctured but interleaved. The length of the blocks of coded bits is $n_t.m.T_{coh}$. The effective rate of the code is $R_e = \frac{R.n_t.m.T_{coh}+2.(L-1).n}{n_t.m.T_{coh}}$. We use an interleaver to break the memory of the code before mapping the coded bits

$\{c_0, \ldots, c_{n_t.m.T_{coh}}\}$. The channel is a MIMO channel that can be ergodic or not, with white complex Gaussian noise η, we suppose here $n_r = n_t = 2.n_s$ antennas in emission and reception to simplify the notations. The $(n_r \times n_t)$ channel complex matrix G is supposed to have independent, zero-mean Gaussian entries with variance 1/2. Equivalently, each entry of G has uniformly distributed phase and Rayleigh distributed magnitude, with expected magnitude square equal to unity. This models a Rayleigh fading channel with enough separation within the receiving antennas and transmitting antennas to achieve independence in the entries of G. A Gray code and an n_t-dimensional M-QAM constellation are used to map the coded bit flow into points of the constellation. The spectral efficiency of the system is $m = log_2 M$ bits per 2-dimension. Each modulated point corresponds to a length-$m.n_t$ vector of coded bits. A scheme of the transmission system is presented on Fig. 23. In this section, we present how to iteratively decode the received signals with probabilities calculus on the exhaustive list of the $2^{m.n_t}$ possible vectors: $\forall i = 1..2^{m.n_t}, \quad c^i = \{c^i_0, \ldots c^i_{m.n_t-1}\}$. There is a probability exchange between the list decoder and the turbo-code decoder. The letter l affects a variable concerning the list decoder, c affects a variable concerning the decoder. We calculate the extrinsic probability ξ_l and a posteriori probability (APP_l) of each coded bit c_j, from the list. By marginalizing the conditional density of probability, we can find the ξ_l value of each coded bit and place it at the input of a SISO decoder for the RSC code, these $\xi_l = obs_c$ values are now named observations. We use a SISO decoder to calculate the APP_c values of the information bits. A hard decision on the APP_c values of the information bits provides an output of the system. At the first iteration, we do not have any information on the coded bits, the a priori probabilities π_c are all equal to 1/2. We can use an iterative method to improve the performance of the above system by re-injecting the extrinsic probabilities ξ_c as new a priori probabilities π_l in the marginalization of the list. We can see this system in the Fig. 4.3.6. The connexions between the three SISO decoders (one for the list and one for each RSC) are described in Fig. 29.

Finally, Figure 30 shows the achievable information rate for 4×4 multiple antenna channel with 16-QAM input alphabet. The mutual information value of 8.0 bits per channel use yields a minimum achievable signal-to-noise ratio equal to 4.0dB. The capacity limit with a Gaussian input at 8.0 bits per channel use is 3.7 dB. Figure 30 illustrates two scenarios: 1- A target list size $N_p = 1000$. The effective list size was distributed between $N_e(min) = 256$ and $N_e(max) = 2300$ with an average equal to 1000. 2- A target list size $N_p = 60000$! The effective list size was distributed between $N_e(min) = 4000$ and $N_e(max) = 26000$ with an average equal to 10000. It is clear that mutual information evaluation is useful at high coding rates ($R_c \geq 1/2$) where its value diverges from the gaussian input capacity. A reduced size list is sufficient in this region. Similarly, Figure 31 shows the achievable information rate for 8×8 multiple antenna channel with 16-QAM input. Figure 32 illustrates the performance of the 4-state parallel turbo code described above. The BICM interleaver size is 20000 and 100000 coded bits respectively. The total number of performed detection/decoding iterations in the BICM receiver is 25. The two different list constructions are also presented, the list centered on y and the list centered on x_{ML}. The performance curve to the most left shows a BER of 10^{-5} at 1.25dB from capacity limit under the constraint of a 16-QAM input.

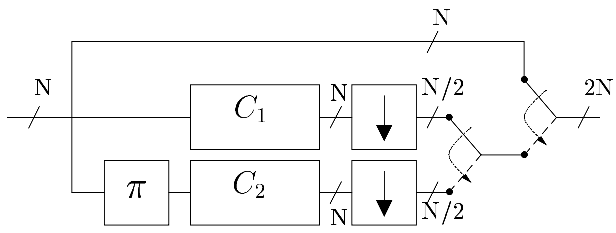

Figure 28: Parallel turbo encoder scheme.

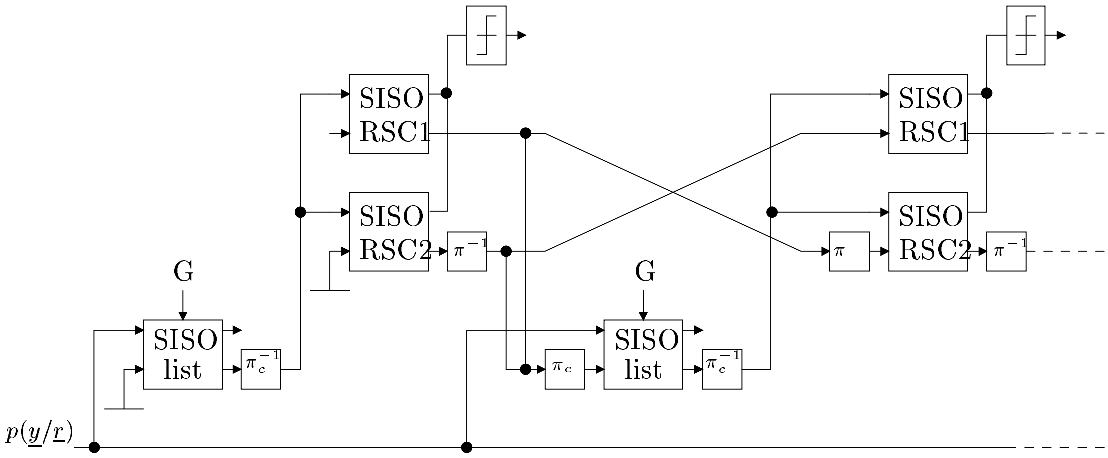

Figure 29: Sequencing of iterative detection and decoding of a Turbo code.

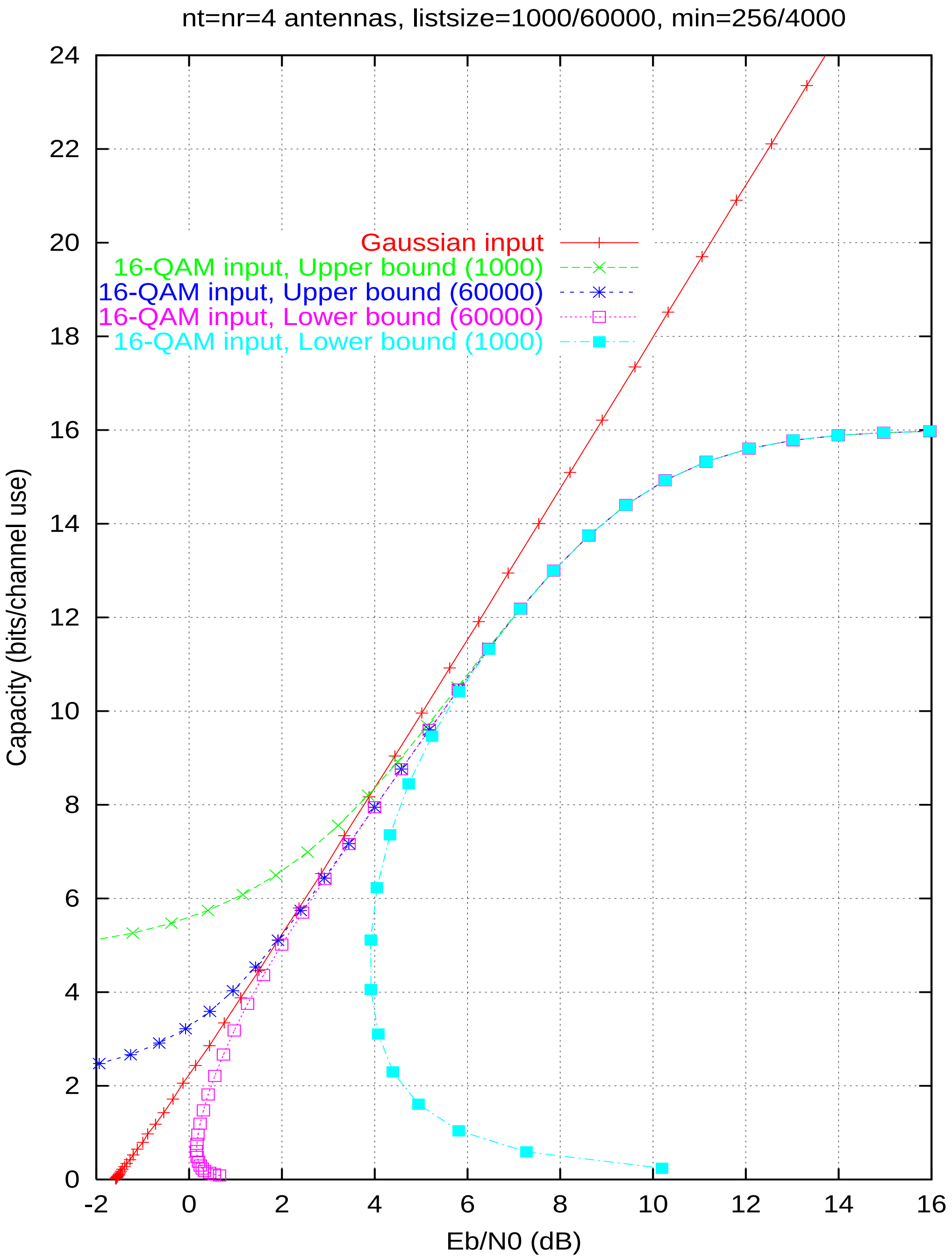

Figure 30: Mutual information evaluation for 4×4 MIMO with 16-QAM

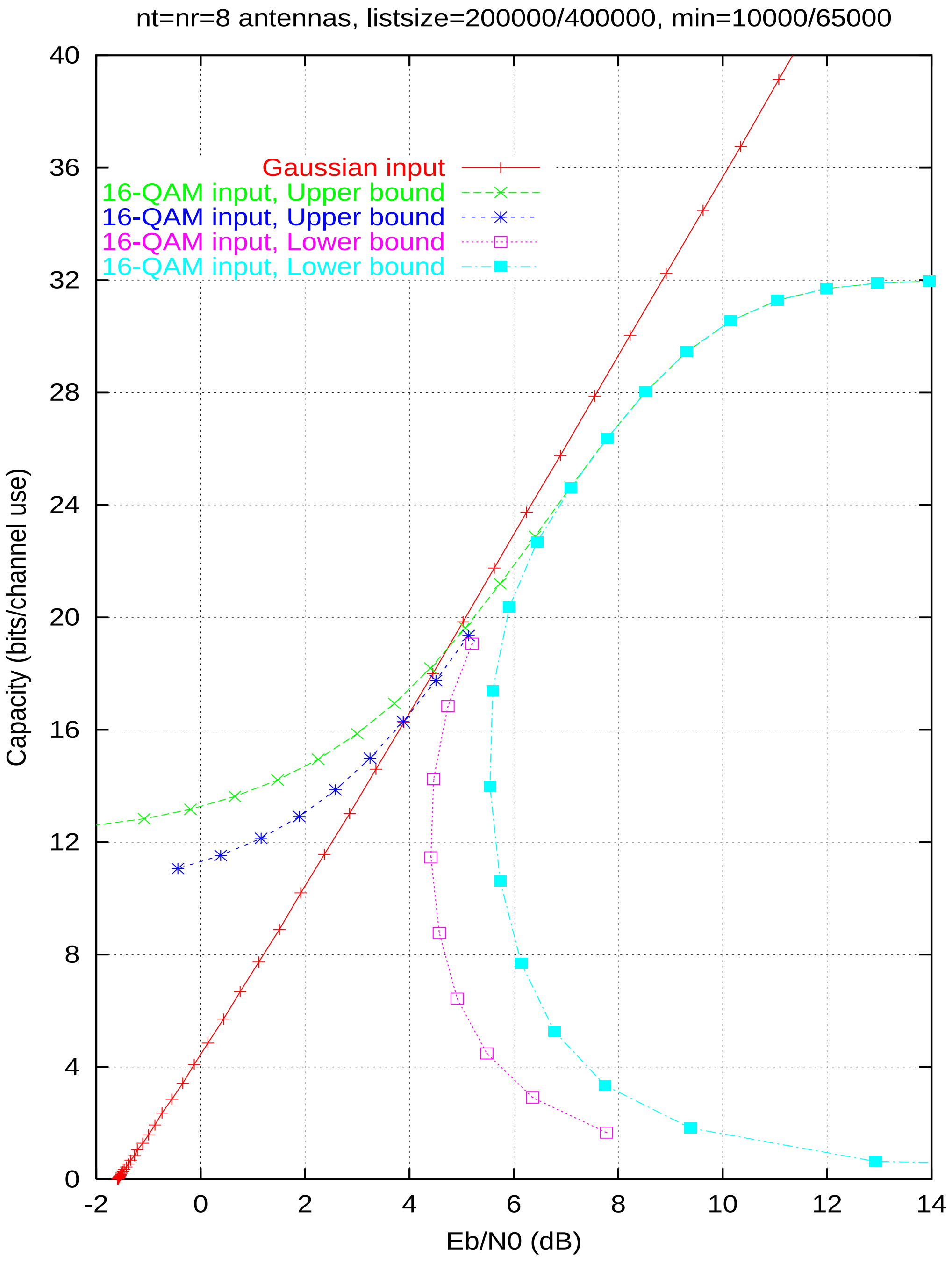

Figure 31: Mutual information evaluation for 8×8 MIMO with 16-QAM

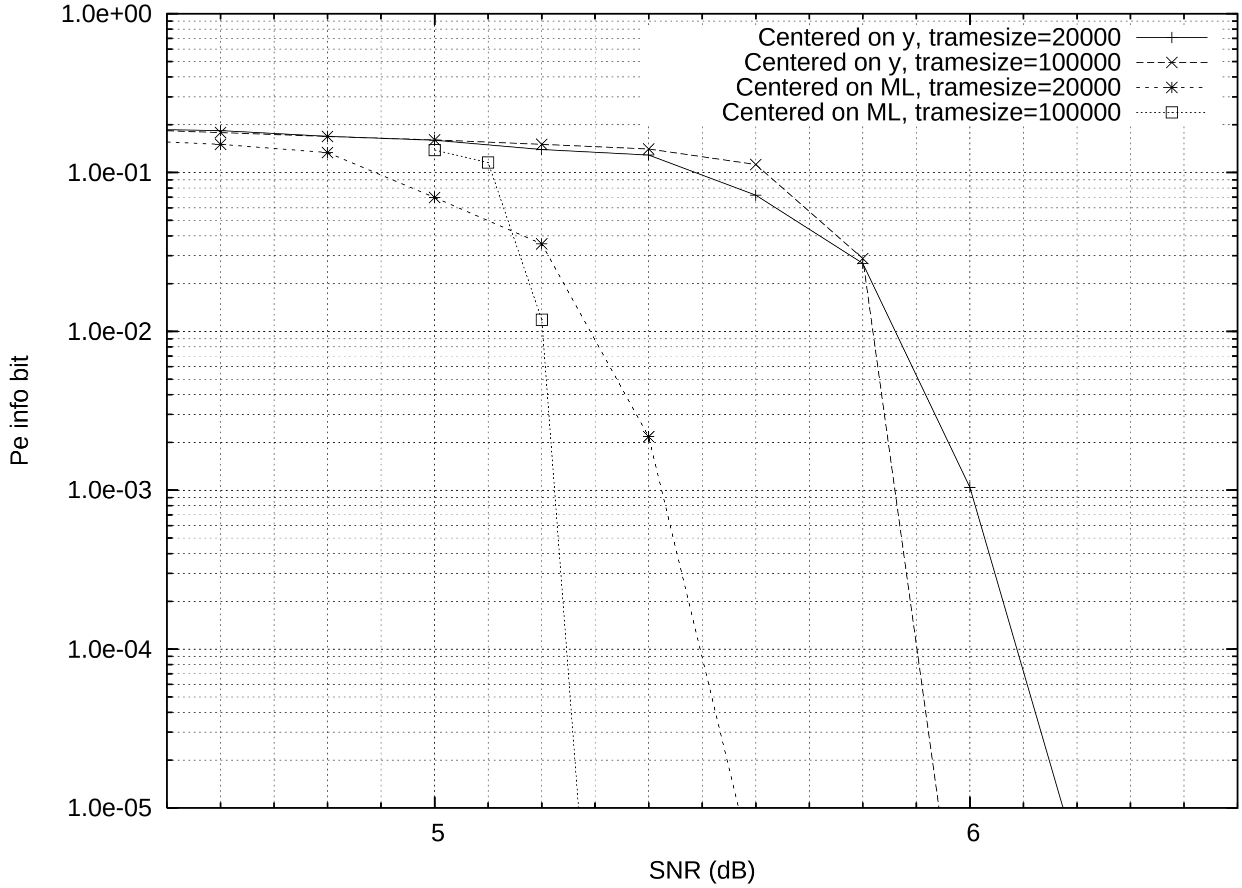

Figure 32: Performance for 4×4 MIMO with 16-QAM, 100000 coded bits interleaver, 4-state turbo-code

5 Conclusions and perspectives

We made an extensive study and a profound analysis of bit-interleaved coded modulations (BICM) considered as space-time codes for multiple antenna channels. On the receiver side, we were able to achieve the following:

- Establishment of a genie bound performance at the detector output.
- Acceleration of the sphere decoder algorithm by taking into account the finite constellation boundaries.
- Invention of a new soft-output sphere decoder where the candidates spherical list is centered around the maximum likelihood point.
- Evaluation of constrained capacity on multiple antenna channels.

On the transmitter side, we were able to achieve the following:

- Optimization of the binary mapping used in QAM constellations.
- Invention of a multi-dimensional mapping from the genie bound.
- Establishment of new design criteria for space-time block codes via the genie bound.
- Construction of a new-space time code from cyclotomic rotations.

We believe that this document contains unprecedented results on channel coding for multiple antennas, e.g., the 1.25dB distance to capacity with 4 transmitting and 4 receiving antennas while transmitting a 16-QAM modulation (see section 4.5). The main conclusion that we state from our results is "**BICM is a universal space-time code**".

Finally, we would like to encourage researchers in this field since many problems are still open. Especially, let us mention the influence of cycles distribution on BICM performance under iterative detection and decoding for finite size interleavers. This problem, if resolved, will help to explain many mysterious phenomena in turbo coding (including LDPC codes on gaussian channels) with and without multiple antennas.

References

[1] E. Agrell, T. Eriksson, A. Vardy and K. Zeger, "Closest point search in lattices," *IEEE Trans. on Information Theory*, pp. 2201-2214, Aug 2002.

[2] S.M. Alamouti, "A simple transmit diversity technique for wireless communications", *IEEE Journal on Selected Areas in Communications*, vol. 16, pp. 1451 -1458, Oct. 1998.

[3] L.R. Bahl, J. Cocke, F. Jelinek, J. Raviv, "Optimal decoding of linear codes for minimizing symbol error rate," *IEEE Trans. on Information Theory*, vol. 20, pp. 284–287, March 1974.

[4] G. Battail, "Théorie de l'Information," Editions Masson, Collection Pédagogique de Télécommunications, 1997.

[5] S. Benedetto, E. Biglieri, V. Castellani "Digital Transmission Theory," Prentice-Hall, Englewood Cliffs, New Jersey, 1987, Also the new.

[6] S. Benedetto, G. Montorsi, D. Divsalar, F. Pollara, "Serial concatenation of interleaved codes: Performance analysis, design and iterative decoding," *TDA Progress Report 42-126*, JPL, August 1995.

[7] C. Berrou, A. Glavieux, P. Thitimajshima, "Near Shannon limit error-correcting coding and decoding: turbo-codes," *Proceedings of ICC'93*, Genève, pp. 1064-1070, Mai 1993.

[8] C. Berrou and A. Glavieux, "Near optimum error correcting coding and decoding: Turbo-codes," *IEEE Transactions on Communications*, vol. 44, pp. 1261–1271, October 1996.

[9] E. Biglieri, D. Divsalar, P.J. McLane, M.K. Simon, "Introduction to trellis coded modulation with applications," new York, Macmillan, 1991.

[10] J. Boutros, "Lattice codes for Rayleigh fading channels," Thèse de Doctorat, ENST, Paris, June 1996.

[11] J. Boutros, E. Viterbo, "Signal space diversity: a power and bandwidth efficient diversity technique for the fading channel," *IEEE Transactions on Information Theory*, vol. 44, pp. 1453–1467, July 1998.

[12] J. Boutros, F. Boixadera and C. Lamy, "Bit-interleaved coded modulations for multiple-input multiple-output channels," proceedings of the *IEEE 6th International Symposium on Spread Spectrum Techniques & Applications*, New Jersey, September 2000.

[13] L. Brunel, "Optimum multiuser detection for MC-CDMA systems using sphere decoding," *PIMRC'01*, San Diego, California, October 2001.

[14] L. Brunel, "Optimum and sub-optimum multiuser detection based on sphere decoding for Multi-Carrier Code Division Multiple Access systems," ICC'02, New York, Apr. 2002.

[15] L. Brunel and J. Boutros, "Lattice decoding for joint detection in direct sequence CDMA systems," *IEEE Transactions on Information Theory*, April 2003.

[16] G. Caire, G. Taricco, E. Biglieri, "Bit-interleaved coded modulation," *IEEE Trans. on Inf. Theory*, vol. 44, no. 3, May 1998.

[17] A. Chindapol and J.A. Ritcey, "Design, analysis, and performance evaluation for BICM-ID with square QAM constellations in Rayleigh fading channels," *IEEE journal on selected areas in commuications*, vol.19, no.5, May 2001.

[18] A. Chouly, A. Brajal, S. Jourdan: "Orthogonal multicarrier techniques applied to direct sequence spread spectrum CDMA systems," *Proc. of GLOBECOM'93*, pp. 1723-1728, Nov. 1993.

[19] J. H. Conway, N. J. Sloane, "Sphere packings, lattices and groups," 3rd edition, 1998, Springer-Verlag, New York.

[20] T.M. Cover, J.A. Thomas, "Elements of Information Theory," John Wiley & Sons, 1991.

[21] K. Fazel, L. Papke: "On the performance of convolutionally-coded CDMA/OFDM for mobile communication system," *Proc. of PIMRC'93*, pp. 468-472, Sept. 1993.

[22] G. J. Foschini, Jr. and M. J. Gans, "On limits of wireless communication in a fading environment when using multiple antennas," *Wireless Personal Communications*, vol. 6, no. 3, pp. 311–335, March 1998.

[23] R.G. Gallager, "Low-density parity-check codes," MIT Press, 1963.

[24] R.G. Gallager, "Information Theory and Reliable Communication, Wiley," New York, 1968.

[25] B. Hochwald and S. ten Brink, "Achieving near-capacity on a multiple-antenna channel," submitted to the *IEEE Transactions on Communications*, July 2001.

[26] H. Imai, S. Hirakawa: "Multilevel coding method using error-correcting codes," *IEEE Trans. on Information Theory*, vol. 23, pp. 371-377, 1977.

[27] H. Jafarkhani, "A quasi-orthogonal space-time block code," *IEEE Trans. on Communications*, vol. 49, PP. 1-4, Jan. 2001.

[28] A.N. Korkin and E.I. Zolotarev. "Sur les formes quadratiques," *Math. Ann.*, vol. 6, pp. 366-389, 1873.

[29] F. Kschischang, B. Frey, H.-A. Loeliger, "Factor graphs and the sum-product algorithm," *IEEE Transactions on Information Theory*, vol. 47, no. 2, February 2001.

[30] A. Lenstra, H. Lenstra Jr., and L. Lovasz. "Factoring polynomials with rational coefficients," *Mathematische Annalen*, vol. 215, pp.515-534, 1982.

[31] X. Li, J.A. Ritcey, "Bit-interleaved coded modulation with iterative decoding," *IEEE Communications Letters*, vol. 1, no. 6, November 1997.

[32] M. Pohst, "On the computation of lattice vectors of minimal length, successive minima and reduced bases with applications," *ACM SIGSAM Bull.*, vol. 66, pp.181-191, 1994.

[33] J.G. Proakis, "Digital Communications," 3rd edition, McGraw-Hill, New York, 1995.

[34] T.J. Richardson, R.L. Urbanke, "The capacity of low-density parity-check codes under message-passing decoding," *IEEE Transactions on Information Theory*, vol. 47, no. 2, February 2001.

[35] C.P. Schnorr and M. Euchnerr, "Lattice basis reduction: improved practical algorithms and solving subset sum problems," *Mathematical Programming*, vol.66, pp.181-191, 1994.

[36] C.E. Shannon, "A Mathematical Theory of Communication," Bell Systems Technical Journal, vol. 27, July and October 1948.

[37] A. Stefanov, T.M. Duman, "Turbo-coded modulation for systems with transmit and receive antenna diversity over block fading channels: system model, decoding approaches, and practical considerations," *IEEE Journal on Sel. Areas in Comm.*, vol. 19, pp. 958-968, May 2001.

[38] R.M. Tanner: "A recursive approach to low complexity codes," *IEEE Trans. on Information Theory*, vol. IT-27, September 1981.

[39] V. Tarokh, N. Seshadri and A. R. Calderbank, "Space-time codes for high data rate wireless communication: Performance criterion and code construction," *IEEE Transactions on Information Theory*, vol. 44, no. 2, pp.744–765, March 1998.

[40] V. Tarokh, H. Jafarkhani, A.R. Calderbank, "Space-time block codes from orthogonal designs," *IEEE Trans. on Inf. Theory*, vol. 45, pp. 1456-1467, July 1999.

[41] E. Telatar, "Capacity of multi-antenna gaussian channels," *Technical report, AT&T Bell Laboratories*, 1999.

[42] G. Ungerboeck: "Trellis-coded modulation with redundant signal sets, Part II," *IEEE Communications Magazine*, vol. 25, no. 2, Feb. 1987.

[43] A.J. Viterbi, J.K. Omura, "Principles of Digital Communication and Coding," McGraw-Hill, New York, 1979.

[44] E. Viterbo and E. Biglieri, "A universal lattice decoder," *Proceedings of 14ème Colloque GRETSI*, Juan-les-Pins, pp. 611-614, Sept. 1993.

[45] E. Viterbo and J. Boutros, "A universal lattice code decoder for fading channels," *IEEE Trans. on Information Theory*, pp. 1639-1642, July 1999.

[46] U. Wachsmann, R.F.H. Fischer, J.B. Huber, "Multilevel codes: theoretical concepts and practical design rules " *IEEE Trans. Inform. Theory*, vol. 45, pp. 1361-1391, July 1999.

[47] J.M. Wozencraft, I.M. Jacobs, "Principles of Communication Engineering," Wiley, New York, 1965.

[48] N. Yee, J.P. Linnartz, G. Fettweis: "Multicarrier CDMA in indoor wireless radio networks," *Proc. of PIMRC'93*, Yokohama, pp. 109-113, Sept. 1993.

[49] E. Zehavi, "8-PSK trellis codes for a Rayleigh channel," *IEEE Transactions on Communications*, vol. 40, pp. 873-884, May 1992.